



ELSEVIER

Deep-Sea Research II 52 (2005) 1246–1269

DEEP-SEA RESEARCH
PART II

www.elsevier.com/locate/dsr2

On the probability of wave breaking in deep waters

Y.A. Papadimitrakis

Water Resources, Hydraulics and Maritime Engineering Division, School of Civil Engineering, National Technical University of Athens, Athens 15780, Greece

Accepted 17 January 2005

Abstract

An analytical expression for the spectral probability density $p_B(\Sigma)$ of breaking waves in deep water, with or without swell, is derived on the basis of a joint distribution of wave frequencies and amplitudes, and a modified Banner and Phillips [1974. *Journal of Fluid Mechanics* 66, 625–640] breaking criterion. The joint probability density and the derived marginal amplitude, frequency and conditional densities, when normalized properly, all show (within the proper spectral bandwidth range) similarities with other pertinent distributions. The derived breaking probability is found to depend on the spectrum bandwidth, θ , and consequently on the significant slope, ξ , and/or the wave age, c_p/u_* , and is not restricted to narrow-band seas. The variation of breaking probability, with ξ , at the normalized spectral peak frequency Σ_p has no direct dependence on c_p/u_* , whereas its counterpart variations at frequencies $2\Sigma_p$, and $2.5\Sigma_p$ both show weak dependence on the latter parameter for large values of wave age (representing mature wave fields), in accord with field observations. An overall (average) breaking probability, B , characterizing the wave field (locally) also is derived and compared with counterpart-published expressions, and their similarities and differences are properly discussed.

© 2005 Elsevier Ltd. All rights reserved.

1. Introduction

Wave breaking is an interesting phenomenon with important implications in studies of the dynamics of the upper ocean, in coastal engineering, remote sensing, meteorology and, perhaps, in some other disciplines, as many of the processes taking place across the ocean–air interface are significantly altered in its presence (Melville, 1996). It is known, for example, that wave breaking

enhances the exchange of gas, water vapor, momentum and energy between the atmosphere and the ocean. It is also known that it has a significant impact on the airflow above waves and, consequently, on the surface drag and the transfer of energy to waves. Sea-surface photographs do show a clear association between breaking waves and the accompanying airflow separation (Banner and Melville, 1976). Wave breaking is also responsible for much of the acoustic noise generated at the ocean surface. Furthermore, it represents the major source of turbulence production in the

E-mail address: ypapadim@central.ntua.gr.

surface layer beneath an air–sea interface, and the primary mechanism of wave energy dissipation. The latter is less known among the processes governing the generation, growth (or decay) and propagation of ocean waves, including the interactions among the various spectral components of the sea surface. For all of the above reasons, it is important to know how often and under what conditions wave breaking occurs.

In deep water, wave breaking maybe caused by various mechanisms, as for example by the non-linear modulations and distortions of the various frequency components of the wave spectrum (Waseda and Tulin, 1999; Tulin and Waseda, 1999; Banner and Tian, 1998; Thorpe, 1995; Banner and Peregrine, 1993; Tulin and Li, 1992; Rapp and Melville, 1990; Dold and Peregrine, 1986). Although the effects of non-linearity on single deterministic wave trains have been studied in the laboratory, the results so obtained have rather limited applicability to the real ocean. In a random sea breaking (and white capping) occur(s) intermittently, owing to the grouping of higher waves and the difference between phase speed and group velocity. In the presence of long waves, the short waves riding the long ones are compelled, by the orbital compression of the long waves, to steepen and possibly break near the long wave crests. Breaking of the front face of a steep gravity wave also may be initiated by the generation of parasitic capillary waves near the crest of the gravity wave (Longuet-Higgins, 1963), or by the blocking of capillary-gravity waves (Phillips, 1981).

The subject of surface wave breaking statistics has attracted the interest of various research groups. The available literature is quite extensive, including laboratory and field observations as well as theoretical approaches and numerical simulations of numerous wave-breaking aspects. Most recent work on the subject is that of Banner et al. (2002), Banner and Song (2002), Song and Banner (2001), Duncan (2001), Banner et al. (2000), Gemmrich and Farmer (1999), Nepf et al. (1998), She et al. (1997), and the references mentioned earlier. In some of these and other older works, it is emphasized that the wave breaking probability and other breaking wave statistics can be para-

meterized in terms of non-dimensional fundamental quantities that express a characteristic steepness of the wave field (locally) and/or the coupling of the wind and wave fields.

In this work, a stochastic model is used for calculating the probabilities of deep wave breaking (as a function of frequency), applicable to both narrow—as well as finite-bandwidth sea spectra. This model is based on a joint probability distribution of wave amplitudes and frequencies.

Parameterization of derived quantities, here, is based on the significant slope, ξ , and the wave age, c_p/u_* , u_* and c_p being, respectively, the wind friction velocity and the phase speed of the dominant wave at the spectral peak frequency; the subscript p characterizes quantities that refers (in general) to the spectral peak. The definition of ξ , although known, will be given later.

2. The stochastic model

The joint distribution of amplitude and frequency (or period), as well as some other pertinent distributions, play an important role in the investigation of many statistical properties of sea waves. Many of these joint distributions are based on linear-wave theories and are restricted to narrow-bandwidth spectra. Yuan's (1982) distribution is based on a relationship between the sea-surface elevation, η , and its second time derivative (or vertical acceleration), η'' , at the extreme points below and above the mean water level (MWL). It was obtained by analyzing the geometry of random waves, and is applicable to both narrow- and finite-bandwidth spectra. Our calculations utilize this joint amplitude-frequency density distribution. For narrow-bandwidth seas, Longuet-Higgins (1983) has proposed a similar distribution that reproduces satisfactorily the behavior of oceanic observations, in such cases, but performs poorly for broadband seas.

The derivation of Yuan's (1982) density function is based on Longuet-Higgins (1957) original joint distribution $p(\eta, \eta', \eta'')$ of η , η' and η'' , and a suitable definition of (intrinsic) frequency, σ . The

latter distribution is given as

$$p(\eta, \eta', \eta'') = \frac{1}{(2\pi)^{3/2} m_2^{1/2} \Delta^{1/2}} \exp \left\{ -\frac{\eta'^2}{2m_2} - \frac{1}{2\Delta} (m_4 \eta^2 + 2m_2 \eta \eta'' + m_0 \eta''^2) \right\}, \quad (1)$$

$$\sigma^2 = -\alpha \eta''(t_0) / \eta(t_0), \quad \Delta = m_0 m_4 - m_2^2. \quad (2a, b)$$

Here prime indicates differentiation with respect to time, m_i is the i th moment of the wave spectrum, and t_0 is the time of occurrence of the (sea) surface extrema. In terms of amplitude, h , and frequency, σ , Yuan's (1982) joint probability density, $p(h, \sigma)$, has the form:

$$p(h, \sigma) = a_y h^2 \exp(-b_y h^2), \quad (3)$$

where

$$a_y = \frac{4\sigma^3}{\alpha^2 (2\pi)^{1/2} m_0^{3/2} \sigma_0^4} \frac{1}{(\theta^2 - 1)^{1/2} (\theta + 1)},$$

$$b_y = \frac{1}{2m_0} \left\{ 1 + \frac{\{1 - \alpha^{-1} \{\sigma / \sigma_0\}^2\}^2}{(\theta^2 - 1)} \right\}, \quad (4a, b)$$

$$\theta = (m_0 m_4 / m_2^2)^{1/2}, \quad \sigma_0 = (m_2 / m_0)^{1/2}. \quad (5a, b)$$

Here α is a positive coefficient dependent also on θ , σ_0 and σ_p . Its variation with these three parameters can be found in Appendix A. θ is the ratio of the expected number of wave extrema and that of zero crossings, per unit time. It is also a measure of the spectrum bandwidth and is related to the parameter ε , introduced by Cartwright and Longuet-Higgins (1956), since $\theta^2 = 1 / (1 - \varepsilon^2)$; for a narrow band case $\varepsilon = 1.0$ and $\theta = 1.0$, whereas in the limit of an extremely broadband field ($\varepsilon = 1$) θ becomes unbounded. Eq. (3) involves no limitation on θ . For calculating θ and σ_0 we have used the filtered moments m_i ($i = 0, 2, 4$) according to an expression suggested by Glazman (1986; see also Appendix B).

Longuet-Higgins' (1983) joint amplitude–frequency function, obtained by properly converting wave periods in frequencies (using his definitions of intrinsic and mean frequencies), also may be expressed in a form similar to Yuan's (1982) model

but with different functionals a_y and b_y , namely

$$a_y = \frac{L(v) \sigma^2}{\pi^{1/2} v m_0^{-1} m_1^2},$$

$$b_y = \frac{1}{2m_0} \left[1 + \left\{ 1 - \frac{\sigma m_0}{m_1} \right\}^2 / v^2 \right], \quad (6a, b)$$

where

$$v = [m_0 m_2 / m_1^2 - 1]^{1/2},$$

$$L^{-1}(v) = \frac{1}{2} [1 + (1 + v^2)^{-1/2}]. \quad (7a, b)$$

To arrive at Eqs. (6) one can use: (i) the joint probability density of amplitude, h , and time derivative of the phase χ , given by Longuet-Higgins (1983), (ii) his definitions of local wave frequency, σ , and (iii) a transfer function, namely:

$$p(h, \chi') = \frac{h^2}{(2\pi m_0^2 m_2)^{1/2}} \exp \left[-\frac{h^2}{2} \left(\frac{1}{m_0} + \frac{\chi'^2}{m_2} \right) \right], \quad (8)$$

$$\sigma^2 = -\frac{\eta''(t)}{\eta(t)}, \quad \sigma = \bar{\sigma} + \chi',$$

$$\chi' = \frac{\partial \chi}{\partial t}, \quad \bar{\sigma} = \frac{m_1}{m_0}, \quad (9a, b, c, d)$$

$$p(h, \sigma) = p(h, \chi') |\partial(h, \chi') / \partial(h, \sigma)|. \quad (10)$$

The surface elevation, η , is represented now by the following expression:

$$\eta = \text{Re}\{h \exp\{i(\bar{\sigma}t + \chi)\}\}$$

$$= \text{Re}\{h \exp(i\chi) \exp(i\bar{\sigma}t)\}$$

$$= \text{Re}\{A(t) \exp(i\bar{\sigma}t)\}, \quad (11a, b, c)$$

where both h and χ are real but slowly varying functions of time t . The above model depends only on the three lowest moments m_0, m_1, m_2 of the spectral density, *but requires the narrow-bandwidth spectrum assumption*. This assumption ensures that the complex-valued envelope function $A(t)$ varies slowly compared to the carrier wave $\exp(i\bar{\sigma}t)$, so that the wave crests lie almost on the envelope $\eta = h$, and $|\chi'| \ll \bar{\sigma}$. Eq. (9b) is also a consequence of this narrow-band assumption.

Tzanis (2003) recently produced a numerical algorithm that examines the sea-surface records and generates the short-term joint density of wave

heights and periods and its byproducts (wave height and period distributions) as a function of a correlation coefficient that correlates wave heights and periods. Tzanis's (2003) results (see also Memos, 2002; Memos and Tzanis, 2000), in the form of joint and marginal distributions, cover a wide range of deep (and shallow) sea states, including conditions up to wave breaking that correspond to nearly any bandwidth. These authors have shown that their results compare favorably with field and large-scale laboratory observations. Since Tzanis's (2003) computer code is not readily available, it was felt appropriate to use the analytic expressions of the joint and marginal statistics of wave amplitudes and frequencies derived, in this work, and explore (perhaps qualitatively) their similarities and differences with the corresponding properties in the wave height-period space of Tzanis (2003).

In the following section, we describe the behavior of the joint density distribution given by Eqs. (3)–(5) and the statistical properties of its byproducts.

3. Properties of various probability densities

3.1. Joint density distribution

Introducing the non-dimensional amplitude $H[=h/(2m_0)^{1/2}]$ and the non-dimensional frequency $\Sigma[=\sigma/(\alpha^{1/2}\sigma_0)]$, $p(h, \sigma)$ is written as

$p(H, \Sigma)$, namely:

$$p(H, \Sigma) = \frac{8H^2\Sigma^3}{\pi^{1/2}(\theta^2 - 1)^{1/2}(\theta + 1)} \times \exp\left\{-H^2\left[1 + \frac{(\Sigma^2 - 1)^2}{\theta^2 - 1}\right]\right\}. \quad (12)$$

The maximum value of $p(H, \Sigma)$, p_{\max} , can be found from the conditions $\partial p/\partial H = \partial p/\partial \Sigma = 0$, which provide the point $(H_{\max}, \Sigma_{\max})$ given by the expressions:

$$H_{\max} = \frac{1}{2} \left\{ \frac{\theta^2 - 1}{\theta^2 + 1 - (3\theta^2 + 1)^{1/2}} \right\}^{1/2},$$

$$\Sigma_{\max} = \{-1 + (3\theta^2 + 1)^{1/2}\}^{1/2} \quad (13a, b)$$

and the value p_{\max} , of $p(H, \Sigma)$ at this $(H_{\max}, \Sigma_{\max})$ point, is given as

$$P_{\max} = \frac{2 \exp(-1)}{\sqrt{\pi}} \left[\frac{\theta - 1}{\theta + 1} \right]^{1/2} \frac{[-1 + (3\theta^2 + 1)^{1/2}]^{3/2}}{[\theta^2 + 1 - (3\theta^2 + 1)^{1/2}]}. \quad (14)$$

Figs. 1(A–C) show contour plots of three typical $p(H, \Sigma)/p_{\max}$ distributions for $\theta = 1.2, 1.5$ and 1.7 , respectively. It is clearly seen that the joint density distribution shows some asymmetry with respect to Σ , in general, but in the neighborhood of $\Sigma = 1$ it becomes symmetric about the mean wave frequency ($\Sigma_{\text{av}} = \alpha^{-1/2}$), independently of H . Σ_{av} is defined in Section 3.2. It is also evident that the variation of bandwidth, θ , alters the shape of the normalized contour lines, and the larger the θ the lower the H values over which $p(H, \Sigma)/p_{\max}$

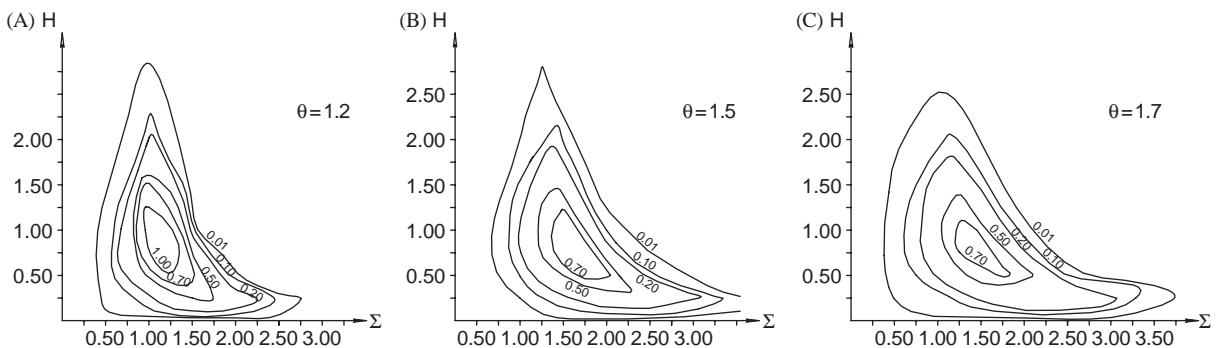


Fig. 1. Typical contour plots of $p(H, \Sigma)/p_{\max}$ distributions for $\theta = 1.2, 1.5, 1.7$: (A) $\theta = 1.2$, (B) $\theta = 1.5$, and (C) $\theta = 1.7$.

Table 1
Parameters of $p(H, \Sigma)$

θ	α	Σ_p	Σ_{\max}	H_{\max}	p_{\max}	Σ_m	Σ_{av}
1.0	0.69	1.00	1.00	1.00	∞	1.00	1.20
1.1	0.65	1.03	1.07	0.95	1.92	1.05	1.24
1.2	0.62	1.06	1.14	0.91	1.40	1.10	1.27
1.3	0.58	1.09	1.21	0.87	1.17	1.14	1.31
1.4	0.56	1.12	1.27	0.84	1.04	1.18	1.34
1.5	0.53	1.14	1.34	0.82	0.95	1.22	1.37
1.6	0.51	1.17	1.40	0.80	0.88	1.26	1.41
1.7	0.48	1.20	1.45	0.78	0.83	1.30	1.44
1.8	0.46	1.22	1.51	0.76	0.79	1.34	1.47
1.9	0.44	1.25	1.56	0.75	0.75	1.38	1.50
2.0	0.43	1.27	1.61	0.73	0.72	1.41	1.53

extends and the greater the width of the Σ values over which $p(H, \Sigma)/p_{\max}$ extends. Comparison of Figs. 1 with counterpart figures of Tzani (2003) shows very good qualitative similarities.

Table 1 lists $\alpha, H_{\max}, \Sigma_{\max}$ and p_{\max} for representative values of the parameter θ between 1.0 and 2.0. Although θ may attain higher values (theoretically, at least), it was felt that the choice $1 \ll \theta \leq 2$ represents realistic broadband field conditions. Table 1 also lists the corresponding values of the normalized peak frequency, $\Sigma_p (= \alpha^{-1/2} \sigma_p / \sigma_0)$, which by virtue of Eq. (A.5) (see Appendix A) is given as: $\{[2 + (4 + 21\theta^2)^{1/2}]/7\}^{1/2}$. The listed values of α correspond to $\sigma_0/\sigma_p = 1.20$ and are typical for values of this ratio between 1.15 and 1.25. It is noteworthy that Glazman (1986) obtained a value of $\sigma_0/\sigma_p (= m_2/m_0)^{1/2} \cong 1.22$ using his filtered zero- and second-order spectral moments that were based on a JONSWAP spectral description (for definitions of Σ_m and Σ_{av} see Section 3.2).

Clearly, broadening of the spectrum enhances and reduces, respectively, the ‘most probable’ joint values of the wave frequency and amplitude, and also reduces their maximum joint probability density. For very large values of both H and Σ (i.e. very small values of the joint density), the normalized contours $p(H, \Sigma)/p_{\max}$ become asymptotically tangent to the H and Σ axes.

3.2. Amplitude and frequency probability densities

The density of the wave amplitude H is now obtained by integrating $p(H, \Sigma)$ with respect to Σ

over all positive frequencies, namely:

$$\begin{aligned}
 p(H) &= \frac{8}{(\pi)^{1/2}(\theta^2 - 1)^{1/2}(\theta + 1)} H^2 \exp(-H^2) \\
 &\quad \times \int_0^\infty \Sigma^3 \exp\left\{-H^2 \frac{(\Sigma^2 - 1)^2}{\theta^2 - 1}\right\} d\Sigma \\
 &= \frac{F(B_m)}{(\theta + 1)} 2H \exp(-H^2) \\
 &= \left[\frac{F(B_m)}{(\theta + 1)}\right] p_R(H), \tag{15a, b}
 \end{aligned}$$

where

$$\begin{aligned}
 F(B_m) &= 1 + \operatorname{erf}\left(\frac{1}{B_m}\right) + \frac{B_m}{\pi^{1/2}} \exp\left(-\frac{1}{B_m^2}\right), \\
 B_m &= \frac{(\theta^2 - 1)^{1/2}}{H} \tag{16a, b}
 \end{aligned}$$

and erf denotes the standard error function. Eq. (15) states that the density of H has a Rayleigh-like distribution, but must be corrected by a factor proportional to $F(B_m)$. For large values of H {O(1) or greater than 1.5}, the correction is small. However, when H is of order $(\theta^2 - 1)^{1/2}$ or less than 1.5 (and $\theta > 1$), the correction becomes significant. Clearly for $\theta = 1, p(H)$ becomes precisely Rayleigh {i.e. $p_R(H) = 2H \exp(-H^2)$ }.

The probabilities of occurrence of positive, and of the sum of positive and negative peaks, in the waveform, can also be obtained and written as

$$\begin{aligned}
 p^+(H) &= \left(\frac{2}{\theta + 1}\right) \left[\left[1 + \operatorname{erf}\left(\frac{1}{B_m}\right) \right] H \exp(-H^2) \right. \\
 &\quad \left. + \frac{B_m}{\pi^{1/2}} H \exp\left(-\frac{\theta^2}{B_m^2}\right) \right], \tag{17}
 \end{aligned}$$

$$\begin{aligned}
 p^\pm(H) &= \frac{1}{\theta} \left[\left[1 + \operatorname{erf}\left(\frac{1}{B_m}\right) \right] H \exp(-H^2) \right. \\
 &\quad \left. + \frac{B_m}{\pi^{1/2}} H \exp\left(-\frac{\theta^2}{B_m^2}\right) \right]. \tag{18}
 \end{aligned}$$

For $\theta = 1$, both of these expressions (17) and (18) reduce to the Rayleigh distribution. Note that $\int p^+(H) dH = 1$ and $\int p^\pm(H) dH = 1$.

The three lowest moments of the amplitude density, $p(H)$, found by numerical integration, are shown in Table 2. They are given as

Table 2
Moments of amplitude probability density

θ	p_0	H_{av}	H^2	$H_{av} - 0.5\pi^{1/2}$	$H_{rms}^2 - 1$
1.0	1.000	0.886	1.000	0.000	0.000
1.1	1.000	0.852	0.955	-0.035	-0.023
1.2	1.000	0.826	0.917	-0.061	-0.043
1.3	1.000	0.804	0.885	-0.082	-0.059
1.4	1.000	0.787	0.857	-0.100	-0.074
1.5	1.000	0.771	0.833	-0.115	-0.087
1.6	1.000	0.758	0.812	-0.128	-0.099
1.7	1.000	0.747	0.794	-0.139	-0.109
1.8	1.000	0.737	0.778	-0.149	-0.118
1.9	1.000	0.728	0.763	-0.158	-0.126
2.0	1.000	0.720	0.750	-0.167	-0.134

$$\begin{aligned}
 P_0 &= \int_0^\infty p(H) dH \\
 &= \frac{1}{\theta + 1} \left\{ 1 + (\theta^2 - 1) \left[\frac{1}{\theta} + 2S_0(\theta) \right] \right\} \\
 &\equiv 1,
 \end{aligned} \tag{19}$$

$$\begin{aligned}
 H_{av} &= \int_0^\infty Hp(H) dH \\
 &= \frac{1}{\theta + 1} \left\{ \frac{1}{2} \pi^{1/2} + \pi^{-1/2} (\theta^2 - 1)^{3/2} \right. \\
 &\quad \left. \times \left[\frac{1}{\theta^2} + 2\pi^{1/2} S_1(\theta) \right] \right\} \\
 &= F_1(\theta),
 \end{aligned} \tag{20}$$

$$\begin{aligned}
 H_{av}^2 &= \int_0^\infty H^2 p(H) d(H) \\
 &= \frac{1}{\theta + 1} \left\{ 1 + \frac{1}{2} (\theta^2 - 1)^2 \left[\frac{1}{\theta^3} + 4S_2(\theta) \right] \right\},
 \end{aligned} \tag{21}$$

where

$$\begin{aligned}
 S_0(\theta) &= \sum_{n=0}^\infty (\theta^2 - 1)^{-(n+3/2)} \left(-\frac{1}{2} \right)^n \\
 &\quad \times \left[\frac{1.3.5 \dots (2n+1)}{n!(2n+1)} \right] \\
 &= \int_0^\infty z e^{-z^2(\theta^2-1)} \operatorname{erf}(z) dz,
 \end{aligned} \tag{22}$$

$$\begin{aligned}
 S_1(\theta) &= \sum_{n=0}^\infty (\theta^2 - 1)^{-(n+2)} (-1)^n \left(\frac{n+1}{2n+1} \right) \\
 &= \int_0^\infty z^2 e^{-z^2(\theta^2-1)} \operatorname{erf}(z) dz,
 \end{aligned} \tag{23}$$

$$\begin{aligned}
 S_2(\theta) &= \sum_{n=0}^\infty (\theta^2 - 1)^{-(n+5/2)} \left(-\frac{1}{2} \right)^n \\
 &\quad \times \left[\frac{1.3.5 \dots (2n+3)}{n!(2n+1)} \right] \\
 &= \int_0^\infty z^3 e^{-z^2(\theta^2-1)} \operatorname{erf}(z) dz.
 \end{aligned} \tag{24}$$

For the limiting case $\theta = 1 : H_{av} = \pi^{1/2}/2$ and $H_{rms}^2 = 1$. It is also seen that the rms value of H_{av}^2 , H_{rms}^2 differs from unity by less than 10% only when $\theta < 1.7$. When $\theta = 1.25$, for example, the difference is about 5%. Furthermore H_{av} , or preferably h_{av} , when properly combined with the spectral peak wavenumber k_p to form the product $h_{av}k_p$, a kind of average slope $(hk)_{av}$ representing the whole wave field (locally), it is found that this average slope $(hk)_{av} (= 8.886 \xi F_1(\theta)$, Section 6) has properties confirmed by field observations (see Section 4.3.1).

The marginal density of frequency, Σ , is obtained by integrating $p(H, \Sigma)$ with respect to H over $0 < H < \infty$, namely:

$$p(\Sigma) = 2(\theta - 1) \left\{ \frac{\Sigma}{[\theta^2 - 1 + (\Sigma^2 - 1)^{1/2}]^2} \right\}^3 \tag{25}$$

Note that $\int_0^\infty p(\Sigma) d\Sigma = 1$. These $p(\Sigma)$ distributions have a peak at $\Sigma_m = \sqrt{\theta}$ (the mode of this distribution) with a value $p_m = [1/\{2(\theta - 1)\}]^{1/2}$. For $\theta = 1, p_m = \delta(\Sigma_m - 1)$ where $\delta()$ is the Dirac delta function. Evidently, broadening of the spectrum reduces these maximum frequency density values p_m . The mean of the total density $p(\Sigma)$ can be obtained from the expression $\Sigma_{av} = \int_0^\infty \Sigma p(\Sigma) d\Sigma$ (or its filtered version). However, because the average frequency of zero up-crossings of the mean water level is $\sigma_{av} = (2\pi)^{-1} (m_2/m_0)^{1/2} = (2\pi)^{-1} \sigma_0$ (in Hz),¹ it becomes apparent that, by our definition, the normalized

¹This definition of σ_{av} maybe not valid for a non-Gaussian field.

average frequency, Σ_{av} , is $\alpha^{-1/2}$. This value of Σ_{av} along with Σ_m is also listed in Table 1. Again, broadening of the spectrum enhances both Σ_m and Σ_{av} .

The effects of spectral bandwidth, in the form of v^2 now, on the distributions of wave height and periods also have been addressed by Tayfun (1983). He found that the probability structure of (crest to trough) wave heights is highly dependent on v^2 and shows significant differences with respect to the Rayleigh theory. Note that $v = 0$ corresponds to $\theta = 1$.

3.3. Conditional distribution of wave frequencies

The distribution of normalized frequency Σ at fixed values of the wave amplitude H , $p(\Sigma|H)$, is found on dividing $p(H, \Sigma)$, by $p(H)$, namely:

$$p(\Sigma|H) = \frac{4H\Sigma^3}{\pi^{1/2}(\theta^2 - 1)^{1/2}} \exp\left[-\frac{H^2(1 - \Sigma^2)^2}{(\theta^2 - 1)}\right] \times F^{-1}(B_m). \tag{26}$$

Note that $\int_0^\infty p(\Sigma|H) d\Sigma = 1$. Eq. (26) has local maxima at the points (H_{mx}, Σ_{mx}) where $\partial p(\Sigma|H)/\partial \Sigma = 0$. This condition leads to

$$H_{mx} = \left[\frac{3(\theta^2 - 1)}{4\Sigma_{mx}^2(\Sigma_{mx}^2 - 1)} \right]^{1/2} \text{ or}$$

$$\Sigma_{mx} = \left[\frac{1}{2} \left[1 + \left[1 + 3 \left\{ \frac{\theta^2 - 1}{H_{mx}^2} \right\} \right]^{1/2} \right] \right]^{1/2}. \tag{27a, b}$$

It can be readily shown that the curve defined by either of Eqs. (27a, b) passes through the point (H_{max}, Σ_{max}) given by Eqs. (13a, b). It also can be verified, by inspection of Fig. 1, that where this curve intersects any contour $p(H, \Sigma)/p_{max} = \text{constant}$, the tangent to that contour is parallel to the Σ -axis. This curve is also asymptotic to both the horizontal Σ -axis and the vertical line passing through $\Sigma = 1$, for large values of Σ and H , respectively, and expresses the asymmetry in the distribution of Σ .

4. Wave breaking

4.1. Breaking criterion

In this work, we have adopted Banner and Phillips (1974) breaking criterion defined by the limiting wave amplitude, h_0 , at frequency σ , properly modified to account for drift current and other effects (described below), given as;

$$h_0 = \frac{c^2}{2\alpha_1 g} \text{ for } \sigma \leq \sigma_p,$$

$$h_0 = \frac{c^2}{2\alpha_1 g} \left(1 - \alpha_0 \frac{u_*}{c}\right)^2 \text{ for } \sigma > \sigma_p, \tag{28a, b}$$

where $c(\sigma)$ is the phase velocity of the wave component at frequency σ , α_1 is a numerical constant of $O(1)$, and α_0 represents the ratio of the Eulerian mean surface-drift current, \bar{q}_{we} , and u_* . The constant α_1 accounts for the fact that the downward crest acceleration of the breaking wave is not exactly $0.5g$ but, as indicated by theoretical analysis and experiments, closer to $0.4g$ (see also Appendix C). The coefficient α_0 is about 0.5, but caution must be exercised in selecting its appropriate value, as most of the surface drift current measurements are conducted in a Lagrangian frame. Therefore, the value 0.53 ($= \alpha_{00}$ in general), often quoted in the literature, may not be suitable for our Eulerian calculations. For intermediate wind speeds (i.e. $30 \leq u_* \leq 40$ cm/s), the Lagrangian fraction α_{00} has been found to increase with u_* , but the opposite appears to be true for very high wind speeds (i.e. $40 < u_* \leq 60$ cm/s). More specifically, the data of Wu (1968) and others indicate that:

$$\alpha_{00} \cong 0.53 \text{ for } 0 < u_* \leq 30 \text{ (cm/s),}$$

$$\alpha_{00} \cong 0.0175u_* \text{ for } 30 < u_* \leq 40 \text{ (cm/s),}$$

$$\alpha_{00} \cong -0.004375u_* + 0.875 \text{ for } 40 < u_* \leq 60 \text{ (cm/s).} \tag{29a, b, c}$$

The data of Plant and Wright (1980), as shown in Smith (1986), have a similar behavior in the range $0 < u_* \leq 30$ (cm/s), with an α_{00} value of 0.60, but for $u_* > 30$ cm/s they indicate that α_{00} decreases monotonically with increasing u_* , reaching ≈ 0.33 at $u_* = 100$ (cm/s). The variation of the Eulerian fraction α_0 with wind and sea state is

given by (see also Papadimitrakis et al., 1988):

$$\alpha_0 = \frac{\bar{q}_{we}}{u_*} = \alpha_{00} - 8\pi^2 \xi^2 \left(\frac{c_p}{u_*}\right), \quad \xi = \frac{m_0^{1/2} \sigma_p^2}{2\pi g} \tag{30a, b}$$

Eq. (30a) simply states that the Eulerian (mean) drift (\bar{q}_{we}) is the difference between its Lagrangian counterpart (\bar{q}_{wl}) and the corresponding surface Stokes transport (\bar{q}_s). This (reduced) form of Stokes transport may be readily obtained by noting that, for a monochromatic wave train, $\bar{q}_s = (ak)^2 c$ (Kinsman, 1965), where a and k represent the amplitude and wave number of the monochromatic wave, and converting the above simple relation into a counterpart expression for a spectrum of waves with the aid of an equivalent amplitude (\bar{a}), associated with the sea-surface variance, the wave number at the spectral peak frequency, k_p , and Eq. (30b).

In the presence of a swell, Eq. (28) is properly modified to include the short- and long-wave interactions. Then according to Phillips (1977), h_0 is given by

$$h_0 = \frac{c^2}{2\alpha_1 g} [(1 - m')^2 - (1 + 2m' - 3m'^2)B'], \tag{31}$$

where $m' = \alpha_0(u_*/c)$ and B' is the swell slope. In this case, owing perhaps to the reduced surface roughness, α_{00} has been found to be somewhat greater than 0.53. For dimensionless wave speeds in the range $8 \leq c_p/u_* \leq 26$, α_{00} has been found to increase with the wave age having values between 0.61 and 0.73, being on the average about 0.65 (Cheung, 1985).

It should be pointed out that Eq. (31) is actually valid for $\sigma \geq \sigma_{cr}$, that is, above the frequency σ_{cr} where the interactions of short waves with the swell (or the dominant wave) become important. Phillips (1981) suggested that $\sigma_{cr} = \{[4B'(1 - B')]^{-1}\} \sigma_p$. He also has suggested that, even in the absence of a swell, the modulation, by the dominant wave, of short waves, riding on the dominant wave back and having frequencies greater than σ_{cr} , remains strong. Hence, the limiting amplitudes at those frequencies ($> \sigma_{cr}$) still may be given by an expression similar to Eq. (31) but with B' now replaced by the average

slope of the wave field $(kh)_{av}$, or by B'_{av} , the average value of the long-wave slopes, if more long waves are present in the sea spectrum (see Eq. (A.16) in Appendix E). For frequencies σ_{cr} , one may apply Eq. (28) instead of (31), although it is likely (for the reasons mentioned above, i.e. associated with the presence of a dominant or other long wind-generated waves) that the short- and long-wave interactions may become effective at frequencies much closer to σ_p ; as mentioned before, $(kh)_{av}$ may be taken as the product $h_{av}k_p$, where k_p is corrected for drift current (wave- and wind-induced) and orbital velocity effects.² Utilizing the definitions of ξ and $h_{av} = (2m_0)^{1/2} H_{av} = (2m_0)^{1/2} F_1(\theta)$, it can be shown that $(hk)_{av} = 2\sqrt{2}\pi \xi F_1(\theta)$. Therefore, under all conditions σ_{cr} maybe given as a multiple of σ_p , with a multiplier being a function of either B' (in the presence of a swell) or ξ and c_p/u_* (trough θ) for wind-generated wave conditions.

In non-dimensional form h_0 {i.e., $H_0 = h_0/(2m_0)^{1/2}$ } is given as

$$H_0 = (4\sqrt{2}\pi\alpha_1 \xi)^{-1} \left(\frac{\Sigma_p}{\Sigma}\right)^2 f \quad \text{for } \Sigma \leq \Sigma_p,$$

$$H_0 = (4\sqrt{2}\pi\alpha_1 \xi)^{-1} \left(\frac{\Sigma_p}{\Sigma}\right)^2 f \left[1 - \alpha_0 \left(\frac{c_p}{u_*}\right)^{-1} \times \left(\frac{\Sigma}{\Sigma_p}\right)\right]^2, \quad \text{for } \Sigma > \Sigma_p, \tag{32a, b}$$

where f expresses a measure of the non-linearity of the wave field which, for monochromatic waves, maybe taken as the ratio $(c/c_\ell)^2$, where the subscript ℓ refers to the corresponding linear phase velocity. For a spectrum of waves, f may be expressed in a number of ways, as various investigators have proposed different forms of f . Longuet-Higgins (1975a), for example, proposed the following form of f , viz.:

$$f = 1 + (hk)_{av}^2 + \frac{1}{2}(hk)_{av}^4 + \frac{1}{4}(hk)_{av}^6 - \frac{22}{45}(hk)_{av}^8 + \dots$$

²For a description of these effects on the dispersion relation see Papadimitrakis (1986).

The variation of f with sea state, in terms of the significant slope, also may be derived following an approach similar to that suggested by Longuet-Higgins and Fox (1978), and can be found in Appendix D (see also Appendix E). The incorporation of f in the above expressions of H_0 accounts (only) indirectly for the influence of non-linearity of the wave field on wave breaking; a more precise analysis of these effects on wave breaking is beyond the scope of this work.

The effects of non-linearity of the wave field on the maximum sea-surface displacement also have been addressed by Song and Wu (1999). These authors, based on a second-order random wave theory, found that the distribution of dimensionless wave maxima becomes flatter and its peak value diminishes as the non-linearity of the wave field increases. This finding is consistent with the classical Fig. 4.26 of Phillips (1977), which, reproducing the results of Cartwright and Longuet-Higgins (1956), does show the decrease of the peak of the probability distribution of the height of wave maxima as the spectrum bandwidth, θ , increases (with increasing ξ).

In the presence of a swell and for frequencies greater than Σ_{cr} (the normalized frequency σ_{cr}), Eq. (32b) is properly modified by replacing the expression of the square bracket by: $[(1 - m')^2 - (1 + 2m' - 3m'^2)B']$, in order to account (again) for the short- and long-wave interactions. Now $m' = \alpha_0(u_*/c_p)(\Sigma/\Sigma_p)$.

The limiting amplitude concept, developed by Phillips (1977), is compatible with the kinematical breaking criterion used by other investigators to characterize a breaking crest that requires that for breaking to occur, the crest orbital velocity, augmented by the local drift current, must exceed the phase velocity of the wave at its forward crest. It is also compatible with the limiting slope concept presented in the following section, as limiting amplitudes maybe readily converted into limiting slopes. Limiting wave steepness measures also have been used by various investigators to characterize wave breaking, in both laboratory and field observations (see, for example, Tulin and Li, 1992). Limiting slopes provide a link among the limiting amplitudes and the limiting downward crest accelerations; this link (or transformation), in

turn, allows for a more accurate estimate of the limiting amplitudes via the estimation of coefficient α_1 (see Appendix C).

4.2. Importance of wind drift on wave breaking

The importance of wind drift effects, on the breaking processes, is worth commenting here in the light of Phillips (1977) pertinent analysis. He supported the idea that the influence of drift current on the spectral densities, remote from the peak, is significant and that freely traveling waves with phase speeds less than (the mean value of) the surface drift are completely eliminated from the spectrum. He further argued that, under natural conditions, the long waves present in the spectrum modulate the surface drift and amplify it manifold along the forward side of the long-wave crest. The maximum drift speed is, theoretically, attained at the long-wave crest (with a value depending on the long-wave slope) and causes the shorter waves to break prematurely there, due to the severe reduction of the respective limiting amplitude, a fact consistent with numerous field and laboratory observations. Field experiments also have stressed the appearance of wave breaking near the center of wave groups, indicating that, due to the sporadic and intermittent nature of breaking, breaking does not necessarily occur at all wave crests. For frequencies greater than about $0.25g/\bar{q}_{we} = (0.25/\alpha_0)(c_p/u_*)\sigma_p$, Phillips (1977) has shown that freely travelling waves are erased completely from the spectrum, a conclusion consistent with the findings of Hsu et al. (1982) that the wave field evolves from a (rather bound) non-linear system, at c_p/u_* values of O(1) or less, to a linear system (with free travelling components) at large c_p/u_* values of O(10) or larger (see also Section 4.3.1).

Although in the presence of a swell α_{00} increases (rather slowly) with increasing wave age, α_0 , given now as $\alpha_{00} - B'^2(c_p/u_*)$, may either increase (for small B' and c_p/u_* values) or decrease (for large B' and c_p/u_* values), indicating that the Eulerian surface mean drift may become more or less effective in this case. Yet, in view of the fact that the drift near the forward face of the long-wave crest is augmented significantly (as described previously) and that wave breaking does occur at

this particular location, it is not clear whether the surface drift is less important in this case, and further analysis is warranted. At any rate, the influence of drift current on the processes of surface wave breaking regards mainly the frequency components above the spectrum peak and, consequently, its importance remains.

4.3. Wave slope considerations

We now recast Eqs. (28) and (31) in a slightly different form. In the absence of swell, using the linear dispersion relationship (i.e. $\sigma_\ell^2 = gk_\ell$) and the equality $k/k_\ell = c_\ell/c$, we obtain:

$$s_{\max} = kh_0 = \left(\frac{f}{2\alpha_1}\right) \left[1 - \alpha_0 \left(\frac{c_p}{u_*}\right)^{-1} \times \left(\frac{\Sigma}{\Sigma_p}\right)^2\right]^2 \quad \text{for } \Sigma > \Sigma_p, \quad (33)$$

where $s_{\max}(\Sigma)$ represents the limiting slope at a frequency Σ . A similar expression holds in the presence of a swell.

From the above description, it becomes apparent that the limiting slope at any given frequency, within a spectrum of waves, depends on both ξ and c_p/u_* . The variation of s_{\max} , as function of Σ/Σ_p , is shown in Figs. 2(A–C) for representative values of the wave age and the significant slope. It is seen now that for a given wave age, s_{\max} is reduced considerably at frequencies remote from the spectral peak. However, at a fixed frequency s_{\max} increases with either c_p/u_* or ξ (or both). The variation of s_{\max} , as a function of c_p/u_* and ξ coupled to c_p/u_* {for example: $\xi = 31.74 \times 10^{-3} (c_p/u_*)^{-0.5}$, see Appendix F} and Fig. 2 all show that, for wave trains with an overall steepness $\xi \leq \xi_{\max}$, the limiting (local) slopes, close to the spectral peak, are smaller than $(kh)_{\max} = 0.4432$. It is also obvious that in the absence of drift currents, since the limiting slope is then $s_{\max,0} = f/2\alpha_1$, the absolute local maximum slope may increase with increasing (overall) steepness ξ from about 0.36 to 0.44 (when $\alpha_1 = 1.39$). Such a behavior is consistent with the field observations of Holthuijsen and Herbers (1986).

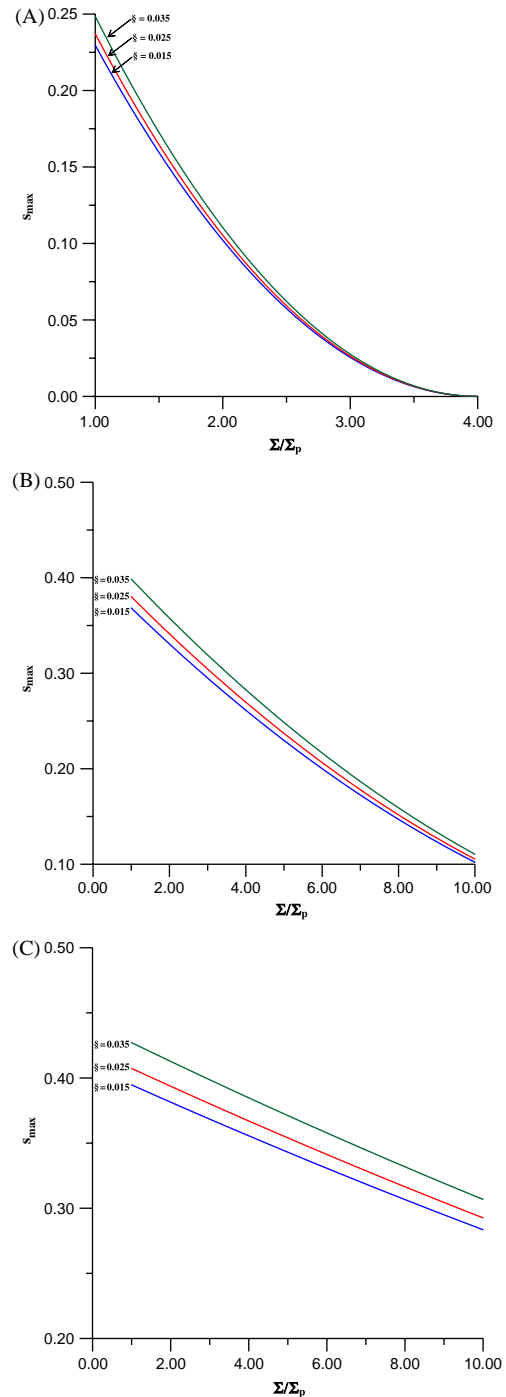


Fig. 2. Typical s_{\max} distributions as a function of normalized frequencies Σ/Σ_p for $\xi = 0.015$ (blue line), 0.025 (red line), 0.035 (green line) and various c_p/u_* values: (A) $c_p/u_* = 2$, (B) $c_p/u_* = 10$, and (C) $c_p/u_* = 30$.

It is worth noting that Ochi and Tsai (1983), in their experiments with unsteady, plunger generated-waves, found signs of breaking individual waves for which $s_{\max} = 0.35$, less than the limiting value of 0.4432, but this is not inconsistent with the fact that the “significant waves”, that is those with amplitude $2\sqrt{m_0}$, cannot have steepness larger than 0.4432. It is also consistent with the fact that the value of maximum wave slope (in the absence of drift current effects), representing also the ratio of downward crest acceleration and g , cannot exceed 0.39.

In the early stages of development of waves generated locally by wind in the absence of a swell, $c_p/u_* \cong 0(1)$ with a typical value of about 2, and $\alpha_0 \cong 0.5$ (as for example, in a laboratory). Then, it appears that wind-drift effects alone reduce the limiting slope, expected otherwise, to about $\frac{1}{2}$ of its value. Low overall steepness also may reduce the maximum real acceleration that the wave crest can reach, before it breaks, and further diminishes the limiting slope at a particular frequency. We therefore can conclude that, unlike Holthuijsen and Herbers (1986), the wave steepness can be used as a parameter to characterize wave breaking, provided that drift current, wave non-linearity, and crest acceleration effects have been properly accounted for. This conclusion also agrees with the findings of Xu et al. (1986) who showed that in (laboratory) wind-waves it is necessary to distinguish at least two classes of breakers—those corresponding to the dominant waves, in the peak of the frequency spectrum, and those corresponding to shorter waves riding on the dominant waves. It is also important to note that Holthuijsen and Herbers (1986) did not consider small-scale breaking (with no air entrainment).

There are other reasons, that also support the contention that the overlapping of the probability density data of the latter authors cannot be used as an exclusive evidence for disputing a wave slope based breaking criterion. Perhaps, the most important among them is the fact that Holthuijsen and Herbers (1986) slope values were deduced from wave-height records during the breaking events, the latter being identified by the presence of white capping. However, it is known that wave slopes attain their maximum value just before, not

during, breaking. As a result of their deduction procedure, waves with a higher slope (prior to breaking) and subsequently breaking are classified as non-breaking events, yielding a biased fraction of unbroken waves on the high side. This explanation provides also a justification for the extremely low mean value of the threshold parameter $(H_f/gT^2) = 0.0067$ reported by the same authors, and referred to in the following Section 4.3.1, as this value apparently contains the bias from many unbroken waves that were considered as breaking (or broken) by the authors. For an explanation of symbols H_f , T see also Section 4.3.1.

In a more recent study Banner et al. (2000), by analyzing the breaking of large-scale dominant surface waves of three geographically diverse natural bodies of water (Lake Washington, Black sea, and the Southern Ocean), concluded that non-linear hydrodynamic processes, associated with wave groups, play an important role in the process of breaking, and that the significant wave steepness is an appropriate parameter to quantify the breaking probability of large-scale waves.

4.3.1. Limiting average wave slope considerations

Lake and Yuen (1978) have found experimentally that for wind waves, generated under a variety of conditions, the average slope $(hk)_{\text{av}} = h_{\text{av}}k_p$ does not exceed 0.28. Then, it can be argued that $\xi \leq 0.28/\{2\sqrt{2}\pi F_1(\theta)\}$. When $\theta = 1$, $F_1(\theta) = \sqrt{\pi}/2$ and $\xi_{\max} = 0.0356$, a value not that different from $\xi = (hk)_{\max}/4\pi = 0.4432/4\pi = 0.0353$. In the previous definition of ξ we have used as amplitude, h , half of the significant wave height (i.e., $2\sqrt{m_0}$) and as a wave number, k , that of the spectral peak; $0.4432\{\pi(H/L)_{\max} = \pi/7.088 \approx \pi/7 = 0.14286\pi\}$ represents the absolute maximum slope value that steady progressive waves can reach at most (cf. Longuet-Higgins, 1985). It is then possible that broadening of the spectrum may cause a reduction in the (max) value of the average slope $h_{\text{av}}k_p\{= 8.886 \xi F_1(\theta)\}$, that the surface-wave configuration can sustain before breaking, such that ξ will not exceed the value of 0.0356. When $\theta = 2$, $F_1(\theta) = 0.72$ and we may expect that, in such a broadband field, the maximum value of $(h_{\text{av}}k_p)_{\max} \approx 0.227$. It is not

unlikely, however, that for higher θ values a somewhat lower value than 0.227 may be attained in the field, as the function $F_1(\theta)$ decreases slowly with increasing θ , approaching a rather constant bound (lower than 0.72). In fact $F_1(\theta)$ approaches 0.61, as θ takes on large values. Recent numerical simulations, as well as field and lab experiments, confirm this finding of reduced maximum average wave slope in broadband wave fields (Banner and Song, 2002; Song and Banner, 2001; Banner et al., 2000; Song and Wu, 1999; Nepf et al., 1998). This finding is also consistent with the conclusions of Song and Wu (1999), provided that the non-linearity of the wave field, f , increases with the wave steepness, ξ , and the bandwidth, θ , increases with ξ . Yet with increasing θ , the height of wave maxima decreases and, therefore, the corresponding limiting slope becomes smaller.

The results of Hsu et al. (1982) also suggest that $(hk)_{av}$ diminishes with increasing non-dimensional fetch and/or wave age. In fact their findings suggest that laboratory (perhaps bound) waves may sustain $(hk)_{av}$ values a little larger than 0.28 [i.e. $(hk)_{av} \approx 0.32$], whereas mature waves in the ocean, with $c_p/u_* \approx 10-20-30$, may attain $(hk)_{av}$ values in the range 0.09–0.06, implying that wind waves evolve from (perhaps) a bound, non-linear system at short fetches to a linear system at large fetches where sea becomes fully developed.

Tulin and Li (1992) also have summarized several limiting steepness measures that characterize breaking waves both in the field and in the laboratory. Their Fig. 3 shows, in an $H_f - gT^2$ graph, the range of dimensionless H_f/gT^2 limiting values that characterize tank experiments (with $H_f/gT^2 = 0.021$), North Sea observations conducted by Holthuijsen and Herbers (1986) (with $H_f/gT^2 = 0.0067$), and the Stokes limit ($= 0.027$). Here H_f is the limiting wave height and T is the corresponding period. Using the dispersion relation, it can be readily shown that these dimensionless H_f/gT^2 limiting values correspond to $H_f/L = 1/7.579, 1/23.75$ and $1/5.89$, respectively, or to ξ values equal to 0.0467, 0.014 and about 0.06. This latter value is somewhat higher than about 0.05 corresponding to the traditional (Stokes) limit of $H_f/L = 1/7$.

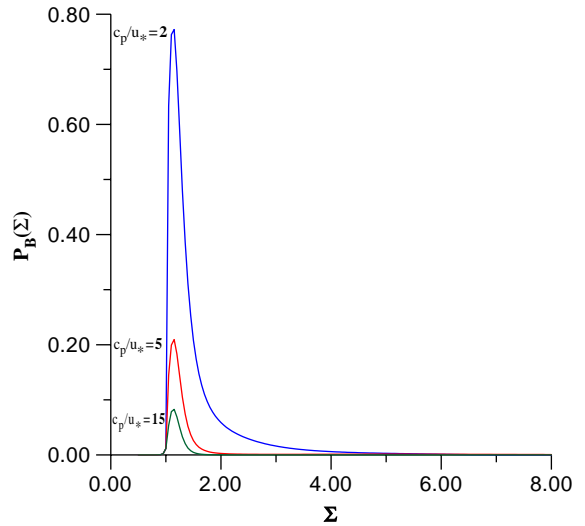


Fig. 3. Typical $p_B(\Sigma)$ distributions in the absence of a swell, expressed by Eq. (36), for various c_p/u_* values and $\xi = 0.02$: (a) $c_p/u_* = 2$ (blue line), (b) $c_p/u_* = 5$ (red line), and (c) $c_p/u_* = 15$ (green line).

The above authors have commented on the large scatter of the laboratory data, and attributed the differences between the laboratory and sea limiting (slope) values to the very different fetches (and the respective different non-dimensional x_* values—for a definition of x_* see Appendix F) encountered in laboratory tanks and at sea (as Hsu et al., 1982, has also suggested). Laboratory wind-waves are characterized by small wave ages of $O(1)$ or less, and they are most likely narrow-banded. Such waves may approach the upper average slope limit, which, however, here appears to exceed Lake and Yuen (1978) bound. Waves at sea, on the other hand, are usually well developed, having wave ages of $O(10)$ or higher, and therefore broad-banded; they can sustain small average slopes. Indeed, for large θ values $F_1(\theta) = 0.61$ and, therefore, $(hk)_{av,min} (= 2\sqrt{2}\pi \xi_{max} 0.61) = 0.193$, an average slope that corresponds to $H_f/gT^2 = 0.0098$. It appears then that the conclusions of Tulin and Li (1992) do not contradict the findings of Hsu et al. (1982), as the value of $H_f/gT^2 = 0.0067$, reported by them to represent an overall field average of breaking wave steepness, corresponds to $(hk)_{av} \approx 0.13$; this latter value is rather consistent

with Hsu et al.'s (1982) expression of $(hk)_{av} = 0.29(c_p/u_*)^{-2/5}$, which, for $c_p/u_* \approx 10$, yields $(hk)_{av} \approx 0.12$. An explanation for this extremely low $(hk)_{av}$ value was offered earlier.

5. Spectral wave breaking probability

The breaking probability, $p_B(\sigma)$, at any frequency σ is obtained by integrating $p(h, \sigma)$ overall positive amplitudes exceeding h_0 , namely:

$$p_B(\sigma) = \int_{h_0}^{\infty} p(h, \sigma) dh. \tag{34}$$

Integration of Eq. (35) with respect to the wave amplitude, h , yields:

$$p_B(\sigma) = [a_y/(2b_y^{3/2})]\Gamma(3/2, b_y h_0^2) \tag{35}$$

or in nondimensional form:

$$p_B(\Sigma) = 4\pi^{-1/2}(\theta - 1)\Gamma(3/2, x_0^2) \times \left\{ \frac{\Sigma}{[\theta^2 - 1 + (\Sigma^2 - 1)^2]^{1/2}} \right\}^3, \tag{36}$$

where

$$x_0 = \left[1 + \frac{(\Sigma^2 - 1)^2}{\theta^2 - 1} \right]^{1/2} H_0. \tag{37}$$

Here $\Gamma(\cdot)$ represents the incomplete Gamma function. *Since the joint model used makes no assumption on the spectrum bandwidth, it is expected that Eq. (36) can cover a wider range of sea states.*

Integration of Eq. (36) over all positive frequencies yields an (overall) average breaking probability of the wave field, $B = B(\xi, c_p/u_*)$, namely:

$$B = \int_0^{\infty} p_B(\Sigma) d\Sigma. \tag{38}$$

Expressions for B , as a function of m_4/g^2 rather than ξ and/or c_p/u_* , also have been proposed by other investigators (Ochi and Tsai, 1983; Snyder and Kennedy, 1983; Srokosz, 1986). Their expressions may be considered similar to Eq. (38), provided that: (a) Σ is a function of H_0 , (b) Eq. (38) can be viewed as an integral (over all crest heights) of the probability that a crest of a given height will break, and (c) as can be

readily shown:

$$\frac{m_4}{g^2} = 4\pi^2 \xi^2 \theta^2 \left(\frac{\sigma_0}{\sigma_p} \right)^4.$$

Ding and Farmer (1994) analyzing field data from the Surface Wave Processes Program in terms of wave breaking statistics, also found that the (average) breaking probability decreases with m_4^{-1} in a (rather) linear statistical fashion (cf. their Fig. 18, although the data scatter in that figure appears to be considerable). Such $B - m_4^{-1}$ behavior is consistent with Srokosz (1986) results (cf. his Figs. 1 and 2), which show that B increases with increasing m_4/g^2 . Then, because m_4 is proportional to both ξ^2 , θ , and the ratio σ_0/σ_p , increases with ξ , it becomes evident that the (average) breaking probability, B , increases rather dramatically with ξ (as our results do show).

Phillips (1985), using action conservation principles, also estimated the average number of (rather large) scale breaking fronts (associated with whitecaps) per unit time and unit area, N_b (in Hz), passing a given point, namely:

$$N_b = \gamma_0 \beta_0^3 b_0^{-1} I(3p) \left(\frac{c_p}{u_*} \right)^{-3} \sigma_p, \tag{39a, b}$$

$$I(p) = \int_{-\pi/2}^{\pi/2} \cos \varphi^p d\varphi,$$

where $b_0 = 0.06$ and β_0, γ_0 are numerical constants that satisfy certain constraints. Since the average number of waves per unit time is $(2\pi)^{-1}(m_2/m_0)^{1/2} = (2\pi)^{-1}\sigma_0$ (in Hz), it follows immediately that Phillips (1985) corresponding average breaking probability, B_{ph} , can be expressed as

$$B_{ph} = 2\pi \gamma_0 \beta_0^3 b_0^{-1} I(3p) \left(\frac{c_p}{u_*} \right)^{-3} \left(\frac{\sigma_0}{\sigma_p} \right)^{-1} \tag{40}$$

with $p = 2$, $\beta_0 = 1.1 \times 10^{-2}$ and $\gamma_0 \beta_0^2 = 0.05$ (cf. Phillips, 1985) we find that:

$$B_{ph} = 0.062 \left(\frac{c_p}{u_*} \right)^{-3} \left(\frac{\sigma_0}{\sigma_p} \right)^{-1}. \tag{41}$$

Phillips transformed expression for B_{ph} (i.e., Eq. (41) does show that the overall breaking probability diminishes with increasing wave age (c_p/u_*), provided that both σ_0/σ_p and f are greater than unity, a behavior in accord with observations

in mature wave fields, since the latter become progressively less steep (gentler, i.e.) with increasing wave age beyond a certain threshold wave age, $(c_p/u_*)_{th}$, of about 1.85.

The dependence of the average breaking probabilities on the wave age also has been stressed by Katsaros and Atakturk (1991) who found that the fraction of spilling and plunging breakers correlates the best with the degree of wave development and the wind stress, not solely with the wave age. A comment on this double parameter dependence of average breaking probability will be offered in Section 6. The similarities and differences among the various expressions of B are also described in Section 6.

6. Results and discussion

Fig. 3 shows typical $p_B(\Sigma)$ distributions in the absence of a swell, as expressed by Eqs. (36) and (37), for various wave ages ($= 2, 5, 15$) and a representative ξ value ($= 0.02$). It is seen from these figures that as the wave age increases and the wave field becomes progressively more mature and broadband, the bandwidth θ increases and the peak breaking probability decreases. As expected, for constant ξ the $p_B(\Sigma)$ curves shrink with increasing wave age, a behavior reflecting precisely the physics of a maturing wave field. If ξ and c_p/u_* (are assumed to) vary independently, then low c_p/u_* values produce peakier breaking probabilities. Fig. 4 shows typical $p_B(\Sigma)$ distributions (in the absence of a swell), for various significant slopes ($= 0.02, 0.025, 0.03$) and a representative wave age (say $= 7$). Again, as expected, for this fixed wave age the peak breaking probability increases with increasing significant slope. $p_B(\Sigma)$ distributions for various wave ages and ξ coupled to them through the ξ - c_p/u_* relation mentioned above (representing wind-generated waves in the absence of a swell) show that as the wave age increases, ξ decreases and the shrinking of $p_B(\Sigma)$ profiles becomes stronger than those when ξ and c_p/u_* vary independently.

Fig. 5A shows the distribution of $p_B(\Sigma_p)$ as a function of ξ , whereas Figs. 5(B) and (C) show typical distributions of $p_B(2\Sigma_p)$ and $p_B(2.5\Sigma_p)$ as a function of ξ and various representative c_p/u_*

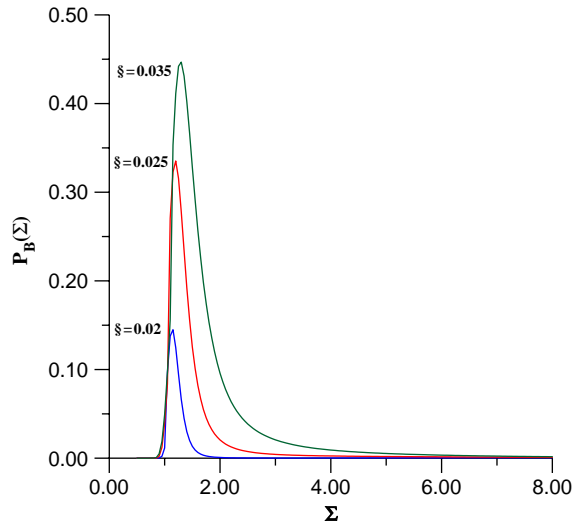


Fig. 4. Typical $p_B(\Sigma)$ distributions, in the absence of a swell, for various ξ values and $c_p/u_* = 7$: (a) $\xi = 0.02$ (blue line); (b) $\xi = 0.025$ (red line); and (c) $\xi = 0.03$ (green line).

values ($= 2, 10, 30$), all in the absence of a swell. It is reminded that since the $p_B(\Sigma_p)$ expression does not depend directly on c_p/u_* , the $p_B(\Sigma_p)$ - ξ curve has no parametric dependence on the wave age. As seen, all of these probabilities increase with increasing ξ and, certainly, the curves showing the distributions $p_B(2\Sigma_p)$ and $p_B(2.5\Sigma_p)$ lie below the $p_B(\Sigma_p)$ curve. It is also apparent that these distributions are less sensitive to the wave age for large values of the latter parameter ($(c_p/u_* \geq 10$, say) representing mainly field conditions, a conclusion virtually in agreement with the findings of Banner et al. (2002) and others.

The variation of B with c_p/u_* , and ξ as a parameter or v.v., as expressed by Eq. (38), is shown in Figs. 6 and 7, respectively, whereas Fig. 8 shows the variation of B as a function of c_p/u_* and ξ coupled to c_p/u_* . As expected (and shown in Fig. 6), B increases with increasing wave steepness, for a fixed value of wave age. B also increases with decreasing wave age, for a fixed ξ value (as shown in Fig. 7). Yet when c_p/u_* and ξ become interdependent (as for waves generated locally in the absence of a swell), the variation of B with c_p/u_* is not monotonic. At very small wave ages B increases with this parameter but

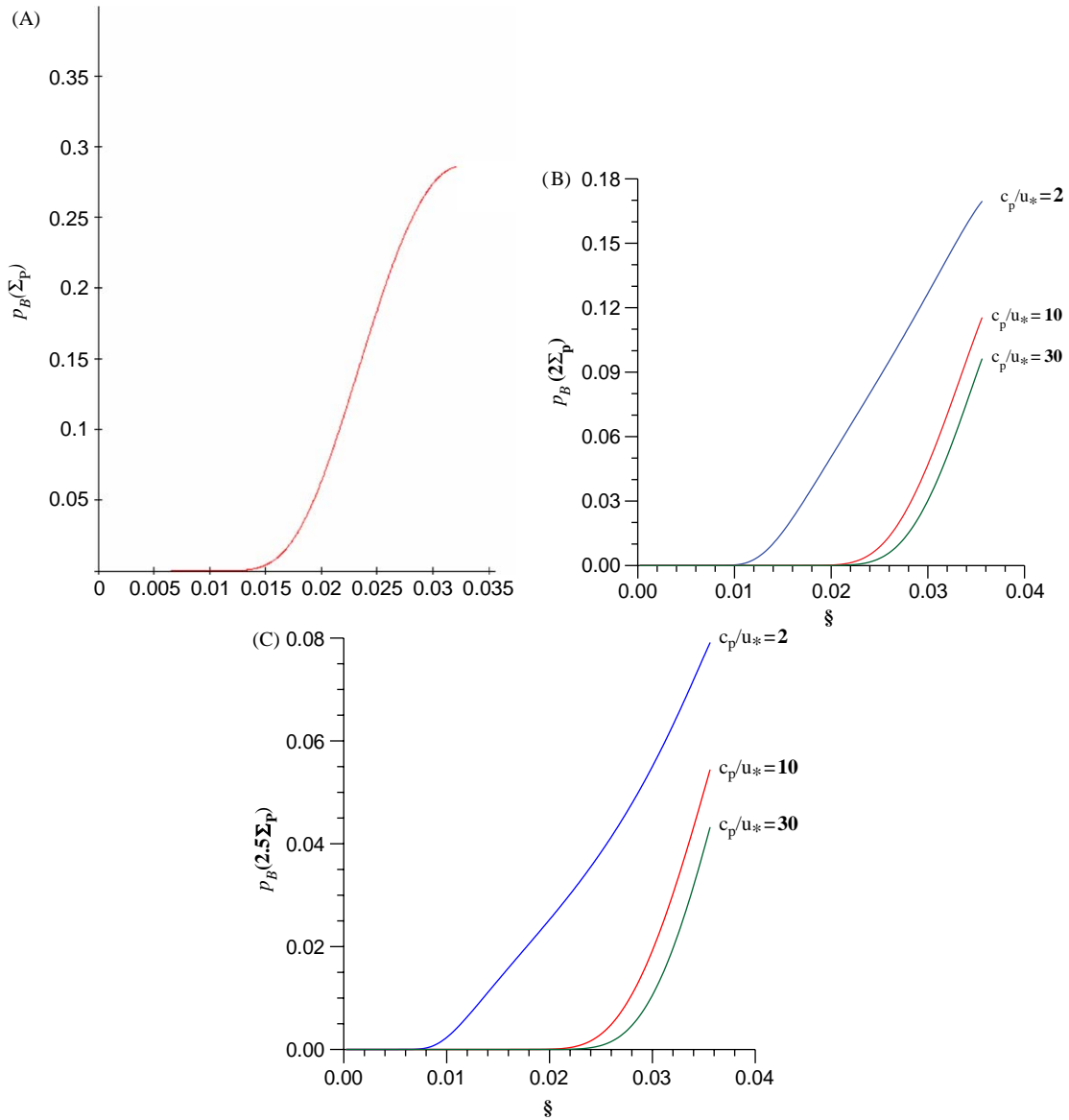


Fig. 5. (A) $p_B(\Sigma_p)$ distribution, in the absence of a swell, as a function of ξ . (B) Typical $p_B(2\Sigma_p)$ distributions, in the absence of a swell, as a function of ξ and various c_p/u_* values ($= 2, 10, 30$); (a) $c_p/u_* = 2$ (blue line); (b) $c_p/u_* = 10$ (red line); and (c) $c_p/u_* = 30$ (green line) and (C) Typical $p_B(2.5\Sigma_p)$ distributions, in the absence of a swell, as a function of ξ and various c_p/u_* values ($= 2, 10, 30$); (a) $c_p/u_* = 2$ (blue line); (b) $c_p/u_* = 10$ (red line); and (c) $c_p/u_* = 30$ (green line) .

beyond the critical value of $c_p/u_* = 1.85 B$ decreases, a behavior in accord with the ascending and descending branches of the ξ - c_p/u_* curve (see also Appendix F).

It is noteworthy that, under conditions where $\xi = \xi(c_p/u_*)$, B also can be expressed as a

function of m_4/g^2 , as given before (Section 5). Since θ varies with both ξ , c_p/u_* ³ (σ_0/σ_p varies rather slowly with these parameters) and now

³As follows from (5a), the definition of significant slope and the dependence of spectral density on c_p/u_* .

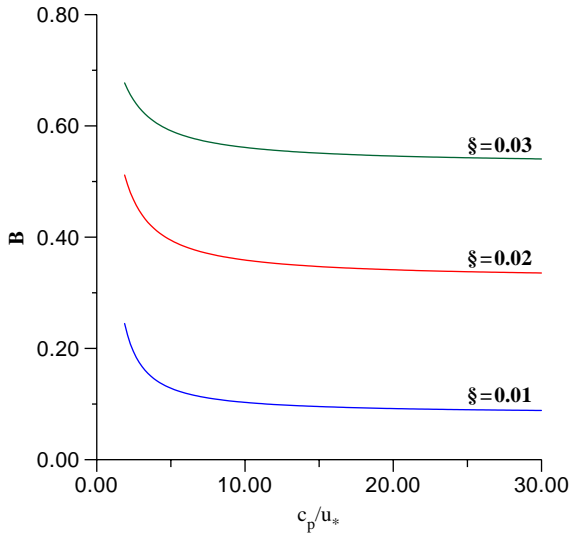


Fig. 6. Typical B distributions, in the absence of a swell, as a function of c_p/u_* and ξ as a parameter, as expressed by Eq. (38): (a) $\xi = 0.01$ (blue line); (b) $\xi = 0.02$ (red line); and (c) $\xi = 0.03$ (green line) .

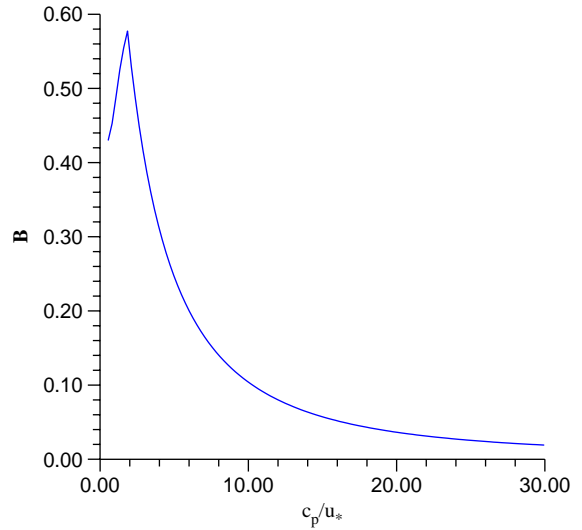


Fig. 8. Variation of B , in the absence of a swell, as a function of c_p/u_* and ξ coupled to c_p/u_* (both branches of the ξ - c_p/u_* curve are represented in this graph).

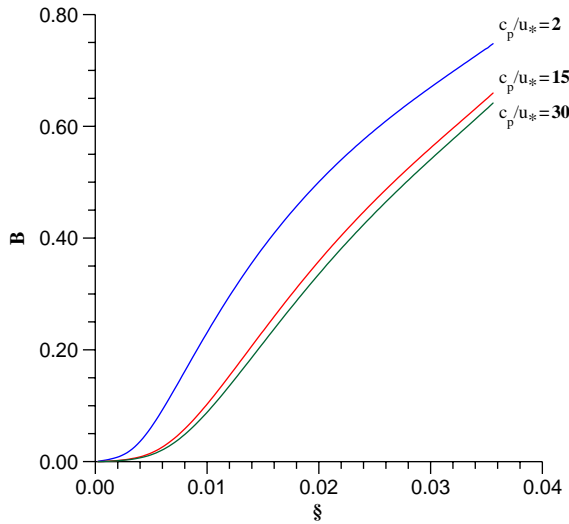


Fig. 7. Typical B distributions, in the absence of a swell, as a function of ξ and c_p/u_* as a parameter: (a) $c_p/u_* = 2$ (blue line); (b) $c_p/u_* = 15$ (red line); and (c) $c_p/u_* = 30$ (green line).

$\xi = \xi(c_p/u_*)$, a unique relation between (say) ξ and m_4/g^2 may be obtained. Furthermore, in order to make the comparison of our B results, given by Eq. (38), consistent with the results of the

respective expression for B given by Srokosz (1986) [i.e. $B_{sr} = \exp[-(\alpha'^2/2)(m_4/g^2)^{-1}]$], we have set the constant of proportionality, α' , appearing in the argument of the latter expression equal to 0.39 (not 0.40), as in Srokosz's calculations the dimensionless limiting downwards crest acceleration was taken equal to 0.4.

The variation of B with ξ , according to Eqs. (36)–(38), Phillips (1985) and Srokosz (1986) expressions, is shown in Fig. 9. As seen, B has similar trends in all cases but its magnitude differs. Our B values are larger than those corresponding to Srokosz (1986) and Phillips (1985) expressions, but this reflects the inclusion of drift currents and other effects in our formulation (only). The latter causes premature breaking at the various frequencies, enhancing the corresponding spectral breaking probabilities and hence B . The fact that our B values are somewhat lower than Srokosz (1986) B , at the higher end of ξ values, maybe explained by noting that his B expression contains contributions from negative peaks as well (not only from the positive ones) and that the number of extrema in a wave form increases at these large wave steepnesses enhancing B more than the inclusion of drift current and other effects could possibly do.

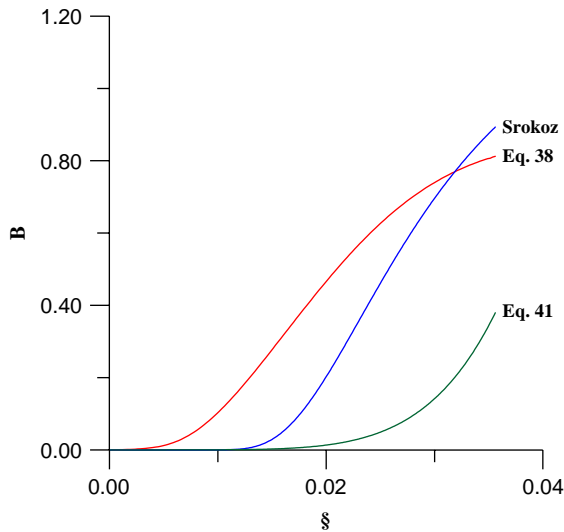


Fig. 9. Variation of B , in the absence of a swell, as a function of S and c_p/u_* coupled to S . Blue, red and green lines represent Srokosz (1986) expression and Eqs. (38) and (41).

Phillips (1985) B curve also lies below the other two curves showing systematically lower B values at any single slope. Such a behavior, however, is not unexpected provided that Phillips expression refers only to (rather) large-scale breaking events associated with the presence of whitecaps, not to all breaking events (i.e. it does not include microbreaking not accompanied by foam formation) and, furthermore, the whitecap fraction or coverage is not identical to breaking probabilities as the former relates to the duration of life of foam (and air bubble formation) while the latter is not.

The fact that the spectral wave breaking probabilities, $p_B(\Sigma)$, and the average breaking probability, B (Eqs. (36)–(38)), depend on both the wave age and the wave steepness appears to support the findings of several field observations that have shown that the spectral breaking probabilities over sufficiently wide frequency bins spread from the spectral peak to about 2.5 times the spectral peak frequency *and/or* the overall breaking probability correlate rather weakly with the wave age alone (Banner et al., 2002; Gemmrich and Farmer, 1999). In many wave fields, it is possible that the significant slope (wave steepness, i.e.) and the wave age may be independent

parameters, particularly if in the area one or more long(er) waves are present, due perhaps to some past storm or other conditions. It is also possible that the poor collapsing of the data sets collected from various observations sites, that some of the earlier mentioned investigators analyzed and subsequently argued that they correlated weakly with the wave age alone, may be due to the fact these fields correspond to waves with and without long waves, conditions that generally require more than one parameter for their description. Nepf et al. (1998) also have argued that wave directionality effects maybe responsible for such discrepancies.

Analytical expressions of various quantities associated with the breaking probability of waves, under different sea state and wind conditions, as for example expressions for the fractional losses of the wave energy per frequency (per unit area and time) and of the total wave-energy losses per average wave cycle (and unit area), caused by deep-wave breaking, as well as expressions of the whitecap coverage and of the turbulence energy dissipation (per unit mass and area, at the sea surface and throughout the water column), as a function of the significant slope and/or wave age, will be given in a forthcoming paper shortly.

7. Conclusions

We have derived an analytical expression for the probabilities of wave breaking (in the absence or presence of swell), as a function of frequency {i.e. Eq. (36)}, using a joint amplitude–frequency probability model that applies to both narrow- and broadband wave fields. The derived expression has incorporated wind forcing, wave non-linearity and downward crest acceleration effects on wave breaking, in the form of a modified Banner and Phillips (1974) mechanism.

The normalized joint density and the derived marginal amplitude and frequency density distributions, as well as the conditional distribution of wave frequencies in the (H, Σ) plane, all show many similarities with their counterpart quantities in the (H, T) plane proposed by Longuet-Higgins (1983), particularly at small θ values (nearly close to unity). The same holds true for contours

of the normalized joint distribution of amplitudes and frequencies $p(H, \Sigma)/p_{\max}$. Our results are also, qualitatively, similar with those of Tzanis (2003).

The maximum value that the average slope, $h_{\text{av}}k_p$, of a surface-wave configuration can attain depends on the spectrum bandwidth, θ , and ultimately on the wave age. It diminishes with increasing wave age, implying that as the wave age increases from very small values of $O(1)$ or less to values of $O(10)$ or larger the wave field evolves from a non-linear (perhaps bound) wave system to a linear one with free traveling waves. The limiting average slope concept provides a means of examining, in a unified manner, field and laboratory observations covering a wide range of wave breaking conditions {as those examined by Tulin and Li (1992)} that correspond to completely different dynamical regimes.

In the absence of a swell, the peak breaking probabilities diminish with increasing wave age at fixed wave steepness and, certainly, increase with increasing steepness at fixed wave age. The breaking probabilities, at normalized frequencies $2\Sigma_p$ and $2.5\Sigma_p$, show a weak dependence on the wave age for large values of the latter parameter (representing mature wave fields), whereas the corresponding probabilities at Σ_p have no direct dependence on the wave age, all in accord with field observations. In the presence of a swell, the breaking probability curves $p_B(\Sigma)$ show a similar behavior, getting peakier as the swell slope B' increases from (typical) values of 0.1–0.3. Yet, they approach nearly zero values close to the spectral peak frequency, much faster than their counterparts curves do in the absence of swell. Due to space limitations, figures associated with breaking probabilities in the presence of swell will be not included here.

The average breaking probability, B (expressed by Eq. (38)), shows a similar behavior (when ξ and c_p/u_* remain independent); it diminishes with increasing wave age, for fixed wave steepness, and increases with increasing steepness for fixed wave age. For large values of wave age, B remains nearly insensitive to the latter parameter. Yet when ξ and c_p/u_* become interdependent (as in wave fields generated locally in the absence of

swell), the variation of B with c_p/u_* is not monotonic; for very small wave ages, on the order of unity or less, B increases with the wave age, but for larger wave ages B decreases with the latter parameter, as expected. The B curves (Fig. 9), representing Srokosz (1986) and Phillips (1985) expressions as a function of wave steepness alone (when c_p/u_* is coupled to ξ through the relationship which describes the descending branch of the ξ - c_p/u_* curve), both have a rising trend similar to the corresponding B curve expressing Eq. (38), although the rates of rising and the B values of these three curves are different. Srokosz (1986) B values are larger in the neighborhood of $\xi = \xi_{\max}$, whereas Phillips (1985) B curve lie below the other two showing systematically lower B values at any single slope.

Appendix A. Determination of α

To determine the coefficient α we define an S -function as

$$S(\sigma) = \frac{1}{2} \int_0^\infty \gamma h^2 p(h, \sigma) dh, \tag{A.1}$$

where $\gamma\{=\gamma(\theta)\}$ is another coefficient with the property $\gamma(1) = 1.0$. From the above definition, it follows that $S(\sigma)$ has dimensions identical to those of the spectral density function; γ accounts for the fact that, for a finite bandwidth spectrum, the expected energy density is not exactly equal to the half of the amplitude squared, as discussed by Longuet-Higgins (1980). Substitution of Eqs. (3)–(5) into Eq. (A.1) yields:

$$S(\sigma) = \frac{3\gamma m_0 \sigma^3}{\alpha^2 \sigma_0^4} \frac{(\theta^2 - 1)^2 (\theta + 1)}{\left[\theta^2 - 1 + \left(1 - \frac{\sigma^2}{\sigma_0^2 \alpha} \right)^2 \right]^{5/2}}. \tag{A.2}$$

It is easily seen now that $S(\sigma)$ is positive definite for all σ values. Since $\int_0^\infty S(\sigma) d\sigma = m_0$, we obtain:

$$\gamma = 2\theta / (1 + \theta) \tag{A.3}$$

For all positive θ , γ increases monotonically with θ . We now force the maximum of the S -function to coincide with the peak of the spectrum. The maximum value of $S(\sigma)$ is readily found from

the condition $\partial S(\sigma)/\partial\sigma = 0$. This yields:

$$\frac{\sigma_{\max}^2}{\sigma_0^2} = \alpha \left\{ \frac{2 \pm \{25 + 21(\theta^2 - 1)\}^{1/2}}{7} \right\}. \tag{A.4}$$

Letting $\sigma_{\max} = \sigma_p$ we find:

$$\alpha = \left(\frac{\sigma_p}{\sigma_0} \right)^2 \frac{7}{\{2 + [25 + 21(\theta^2 - 1)]^{1/2}\}}. \tag{A.5}$$

Theoretically, when $\theta = 1$, α should also be equal to 1; yet according to Eq. (A.5) $\alpha = (\sigma_p/\sigma_0)^2$ which, in general, is not exactly unity. However, calculations with either laboratory or field data show that α is not significantly different from unity (Typically: $\sigma_0/\sigma_p \cong 1.15$ and 1.20 , respectively, for wind-generated waves in the presence or absence of swell).

Appendix B. Low-pass filtering and high-order moments

Filtering is commonly used in signal processing techniques. Its application essentially removes the difficulties encountered in determining m_4 from field and laboratory data, since the high-frequency tail of the measured spectrum is usually quite noisy. Low- and/or band-pass filtering has also been applied to theoretical calculations of group statistics by Longuet-Higgins (1986, 1984). Glazman (1986) presented a filtering technique, which successfully resolves the problem of calculating the high-order moments of the sea spectrum. His technique is based on the theory of random fields (Vanmarcke, 1983) and treats the surface elevation as specified on a spatial (or temporal) running grid. The introduction of a spatial (temporal) scale, characterizing the resolution of a given physical theory (or observational technique) makes the statistical description of the wave field consistent with the limitations of the physical theory that has yielded a given model of sea waves. In this work we have adopted Glazman, 1986 approach in calculating the filtered moments m_i ($i = 0, 1, \dots, 4$) of the wave spectrum. According to him (cf. his Eq. (27)):

$$\begin{aligned} m_0 &= \int_{-\pi}^{\pi} \int_0^{\infty} V^2(\sigma T_f) F(\sigma, \varphi) d\sigma d\varphi, \\ m_1 &= \int_{-\pi}^{\pi} \int_0^{\infty} V^2(\sigma T_f) \sigma F(\sigma, \varphi) d\sigma d\varphi, \\ m_2 &= \int_{-\pi}^{\pi} \int_0^{\infty} V^2(\sigma T_f) \sigma^2 F(\sigma, \varphi) d\sigma d\varphi, \\ m_4 &= \int_{-\pi}^{\pi} \int_0^{\infty} V^2(\sigma T_f) \sigma^4 F(\sigma, \varphi) d\sigma d\varphi, \end{aligned} \tag{B.1a, b, c, d}$$

where

$$V(\sigma T_f) = \sin(\sigma T_f/2)/(\sigma T_f/2), \tag{B.2}$$

T_f and φ are cutoff period and angle of wave propagation direction. Evidently, as $T_f \rightarrow 0$, $V(\sigma T_f) \rightarrow 1$. $F(\sigma, \varphi)$ is the 2D wave spectrum which, in many applications, is approximated by the product of the 1D spectrum, $\Phi(\sigma)$, and a directionality spreading factor, $D(\varphi)$, viz., $F(\sigma, \varphi) = \Phi(\sigma)D(\varphi)$. Occasionally the spreading factor is expressed as $D_1(\sigma, \varphi)$. Then: $F(\sigma, \varphi) = \Phi_1(\sigma)D_1(\sigma, \varphi)$, and integration of this $F(\sigma, \varphi)$ function, over $-\pi$ to π , yields (perhaps) a different $\Phi(\sigma)$. $F(\sigma, \varphi)$ and $D(\varphi)$ must satisfy the conditions:

$$\begin{aligned} &\int_{-\pi}^{\pi} \int_0^{\infty} F(\sigma, \varphi) d\sigma d\varphi \\ &= \int_0^{\infty} \Phi(\sigma) d\sigma = \overline{\eta^2} = \eta_{\text{rms}}^2, \\ &\int_{-\pi}^{\pi} D(\varphi) d\varphi = 1. \end{aligned} \tag{B.3a, b, c}$$

The directional wave spectrum, $F(\sigma, \varphi)$, proposed by Donelan et al. (1985), and modified slightly by Banner (1990), has been used in the subsequent calculations of spectral moments m_i ($i = 0, \dots, 4$).

The application of filter function (B.2) to the spectral density $F(\sigma, \varphi)$ removes from the latter all components with periods shorter than T_f . However here, unlike in Glazman (1986), T_f is not taken as the Taylor (time) microscale defined by $2\pi(m_0/m_2)^{1/2}$. Such a cutoff period corresponds to a frequency σ_f , which lies in the range $\sigma_p < \sigma_f < 2\sigma_p$ and essentially eliminates an important part of the spectrum (i.e. a significant part of the equilibrium region). In this study the cutoff

frequency, σ_f , has been taken as the smaller of $(10\sigma_p, \sigma_v)$, where σ_v represents the threshold frequency that separates the capillary and viscous dissipation regions of the spectrum. It has been suggested that σ_v increases with u_* , and that for wind speeds between 3 and 10 m/s, $45 \times 2\pi (= 283) \leq \sigma_v \leq 200 \times 2\pi (= 1257 \text{ rad/s})$. Komen (1987) also proposed that $\sigma_v = \alpha' u_*^2 / \nu$, where $\alpha' \approx 0.04$ and ν here is the kinematic viscosity of water. We have set $\sigma_v = \max(283, \alpha' u_*^2 / \nu)$. Our cutoff frequency, σ_f , is greater than the value of $5\sigma_p$ used by other investigators in the past, but consistent with photographs of whitecap events showing that σ_f ought to be in the range $(5-10)\sigma_p$.

Appendix C. Determination of α_1

From Eq. (33) it follows that in the absence of drift currents, the limiting slope $s_{\max,0} (= f/2\alpha_1)$ increases monotonically with ξ ; $s_{\max,0}$ also may be taken as the ratio of the real, downward wave crest and gravitational accelerations (α_L and g , respectively), provided that $h_0\sigma^2/g = -f/2\alpha_1$ represents the dimensionless (limiting) downward wave crest acceleration. For waves of arbitrary steepness ($\leq \xi_{\max}$), the variation of $s_{\max,0}$ with ξ can, therefore, be interpreted as that of α_1/g with ξ . Since, however, the calculations of Longuet-Higgins (1985) show that for (symmetric, steady) waves approaching the limiting form $\alpha_L/g \cong -0.39$, it is possible to estimate the numerical coefficient α_1 such that $s_{\max,0} = 0.39$ when $\xi = \xi_{\max}$. This yields: $\alpha_1 = f_m / (2 \times 0.39) = 1.53$, where $f_m (= 1.1931)$ is the value of f corresponding to $\xi = \xi_{\max}$ (see also Appendix D). Somewhat different α_1 values are obtained when α_1 is interpreted as either the ratio of $0.50g/0.39g (= 1.28)$ or when $s_{\max,0} = 0.4432$, which then yields $\alpha_1 = f_m / (2 \times 0.4432) = 1.35$. A similar value of f_m may be obtained if the expression of f , proposed by Longuet-Higgins (1975a) and shown above is used with $(kh) = (kh)_{\max} \approx 0.4432$. That yields: $f_{m,LH} = 1.24$, and the corresponding α_1 values are: $\alpha_1 = f_{m,LH} / (2 \times 0.39) = 1.58$ or $\alpha_1 = f_{m,LH} / (2 \times 0.4432) = 1.39$. In this study α_1 has been taken as 1.39.

Appendix D. Wave field non-linearity considerations

In this study, the phase velocities c have been corrected to account for the non-linearities of the wave field according to the following relationship (Longuet-Higgins and Fox, 1978):

$$f = \frac{c^2}{c_\ell^2} = 1.1931 - 1.18\varepsilon_1^3 \cos(2.143 \ln \varepsilon_1 + 2.22). \quad (\text{D.1})$$

The coefficient ε_1 can be determined as described in Longuet-Higgins (1985, 1986). Briefly, for uniform, steady wave trains, and in the absence of drift currents, ε_1 is given by

$$\varepsilon_1 = \frac{c - u_{\text{orb}}}{\sqrt{2}c_\ell}, \quad (\text{D.2})$$

where u_{orb} denotes the wave crest orbital velocity. Longuet-Higgins and Fox (1978), and Longuet-Higgins (1980) have also shown that ε_1 is a function of the crest wave slope hk , namely:

$$kh = (kh)_{\max} - 0.50\varepsilon_1^2 + 0.160\pi\varepsilon_1^3 \times \cos(2.143 \ln \varepsilon_1 - 1.54), \quad (\text{D.3})$$

where $(kh)_{\max} (\cong 0.4432 = 0.14107\pi)$ is the absolute maximum value of the wave slope. This limiting slope value is in fact the Stokes limit {i.e., $(H_f/L) \approx 1/7$, $\xi_{\text{st}} = 0.0505$ }. For a spectrum of ocean waves (perhaps asymmetric, unsteady wave trains), Eq. (D.3) still can be used to obtain a mean value of ε_1 , if one replaces hk by a characteristic mean slope, say, $h_{\text{av}}k_p$. In terms of the significant slope ξ , Eq. (D.3) can be recast in the form:

$$\xi = [F_1(1)/F_1(\theta)] \xi_{\max}^s - 0.5\{2\sqrt{2}\pi F_1(\theta)\}^{-1}\varepsilon_1^2 + 0.160\pi\{2\sqrt{2}\pi F_1(\theta)\}^{-1}\varepsilon_1^3 \times \cos(2.143 \ln \varepsilon_1 - 1.54) \quad (\text{D.4})$$

ξ_{\max}^s represents the maximum value of the significant slope that corresponds to the Stokes limit (≈ 0.0505). Yet, since this limit is not realized in the field it was considered appropriate to use the limiting value $\xi_{\max} = 0.0356$ found in Section 4.3.1. In utilizing Eq. (D.4), we have assumed that for a spectrum of waves the nonlinear phase velocity can still be determined from an equation

derived for uniform waves by means of a characteristic (average) slope. However, further testing of this hypothesis may be required in the future. Accurate c/c_ℓ values were obtained by successive Pade approximants $[N, N]$, with $N = 15$ (cf. Longuet-Higgins, 1975b), for ξ varying from zero up to ξ_{\max} . In the following appendix we present another approximate expression for the ratio c/c_ℓ , that is for f .

Appendix E

We assume here that the effects of nonlinearity of the wave field on the ratio c/c_ℓ are independent of frequency, that is, $c/c_\ell \cong \bar{c}/\bar{c}_\ell$. Here \bar{c} represents a mean characteristic phase velocity and $\bar{c}_\ell = g/\sigma_0$. Then, from the definition of ε_1 it follows that:

$$\frac{\bar{c}}{\bar{c}_\ell} = \frac{u_{\text{orb}}}{\bar{c}_\ell} + \sqrt{2}\varepsilon_1, \tag{E.1}$$

where ε_1 can be obtained in terms of ξ via Eq. (D.4). The above equation neglects surface drift current effects, and a more complete expression for the ratio \bar{c}/\bar{c}_ℓ may be given as:

$$\frac{\bar{c}}{\bar{c}_\ell} = \frac{u_{\text{orb}}}{\bar{c}_\ell} + \frac{\bar{q}_{\text{we}}}{\bar{c}_\ell} + \sqrt{2}\varepsilon_1. \tag{E.2}$$

Since for a monochromatic wave train, $u_{\text{orb}} \propto h\sigma$, it can be argued that for a spectrum of waves:

$$u_{\text{orb}}^2 = 2 \int_0^\infty V^2(\sigma T_f) \sigma^2 \Phi(\sigma) d\sigma. \tag{E.3}$$

For calculating u_{orb} , in wind-generated waves without swell, a modified Donelan spectrum has been adopted, as described earlier.

In the presence of a swell, a somewhat different form of the spectrum is adopted for frequencies greater than a critical frequency, σ_{cr} , where the interactions of short waves, riding on the swell, with the swell become significant (Phillips, 1977), viz.,

$$\Phi(\sigma)_{\text{sw}} = \Phi(\sigma)\{(1 - m')^2 - (1 + 2m' - 3m'^2)B'\}^2 \tag{E.4}$$

for $\sigma \geq \sigma_{\text{cr}}$.

Under field conditions, it is perhaps more realistic to replace B' either by $(kh)_{\text{av}}$ or by B'_{av} , the average

of the maximum slopes associated with the long waves, in the case of co-existence of more than one long waves in the sea spectrum. According to Longuet-Higgins (1962), for a random Gaussian surface:

$$B'_{\text{av}} \cong \left[2 \int_0^{\sigma_f} V^2(\sigma T_f) k^2 \Phi(\sigma) d\sigma \right]^{1/2}. \tag{E.5}$$

Combining the above expressions, we may write

$$f^{1/2} = \frac{\bar{c}}{\bar{c}_\ell} = 2\sqrt{2}\pi \xi F_c + \alpha_0 \left(\frac{c_p}{u_*} \right)^{-1} F_c^{1/2} - \sqrt{2}\varepsilon_1. \tag{E.6}$$

F_c is a complicated function of ξ , c_p/u_* and of the spectrum characteristics. Comparison of the variation of $f^{1/2}$ with ξ , according to Eqs. (E.6) (with $u_* = 0$) and (D.1), shows satisfactory agreement.

Appendix F. Significant slope-wave age correlations

In order to get a deeper insight into—and a better understanding of—the behavior of the results derived in this study, it was felt appropriate to explore the nature of significant slope–wave age correlations that might exist under field and laboratory conditions, in the absence and/or present of swell. The $p_B(\Sigma)$ and B results may differ (to a greater or lesser extent) depending on whether ξ and c_p/u_* remain coupled or independent, and the extent of similarities or differences of $p_B(\Sigma)$ and B results certainly depends on the combination of the parameters and/or the ξ - c_p/u_* correlation used. In the absence of swell, these two non-dimensional parameters are interdependent, whereas the opposite appears to be true for wind-generated seas in the presence of swell. Yet, in the former case these correlations may also differ under laboratory and field conditions.

In the early stages of development (or at very short fetches) where $c_p/u_* \approx O(1)$ or less, the wave steepness increases with wave age (cf. Fig. 4 of Huang et al., 1986; Fig. 4.19 of Jones and Toba, 2001 taken from Baily et al., 1991), whereas for developing waves (at moderate and large fetches) ξ decreases with it. The field data of Kahma

(1981), for example, indicate that in the latter case $\xi \propto (c_p/u_*)^{-1/2}$, but similar expressions have been proposed by Hsu et al. (1982) and others.

More recent expressions relating ξ (or the mean square slope, $S^* = k_p^2 \eta_{\text{rms}}^2$) with the non-dimensional frequency, σ^* , can be obtained by utilizing the data on dimensionless energy, e^* , frequency, σ^* , and fetch, x^* , reported in Kahma and Calkoen (1994) and in Young (1999). Their studies provide excellent summaries of the efforts made to produce the best correlations of the form: $e^* = A_1 x^{*a}$ and $\sigma^* = B_1 x^{*b}$, where $e^* = \eta_{\text{rms}}^2 g^2 / U_{10}^4$, $\sigma^* = U_{10} \sigma_p / g$, $x^* = gx / U_{10}^2$ and x denotes fetch. Elimination of x^* between these two correlations, recalling that $e^* = S^* \sigma^{*-4}$ and using the average coefficients suggested by Young (1999), yields: $S^* = 2.47 \times 10^{-3} \sigma^{*0.8}$. Since, however, $\xi^2 = S^* / 4\pi^2$, it follows that: $\xi = 7.91 \times 10^{-3} (c_p / U_{10})^{-0.4}$, an expression very similar to that proposed by Donelan et al. (1985), viz.: $\xi = 33.1 \times 10^{-3} (c_p / U_{10})^{-0.35}$. Since also $U_{10} = u_* C_d^{-1/2}$, where C_d is the drag coefficient, it follows immediately that in terms of the wave age c_p / u_* , the first correlation maybe expressed as: $\xi = 7.91 \times 10^{-3} (c_p / u_*)^{-0.4} C_d^{-0.2}$. Several expressions have been proposed for C_d as a function of c_p / u_* , in the form: $C_d = A_2 (c_p / u_*)^{B_2}$, most notably that of Geernaert et al. (1987) who found that $A_2 = 0.0148$ and $B_2 = -0.738$. Substitution of this C_d expression into the above correlation yields: $\xi = 18.37 \times 10^{-3} (c_p / u_*)^{-0.2424}$, a form similar to that proposed by Kahma (1981). For waves, however, developing in rather short fetches, the exponent B_2 in the above expression for C_d maybe positive, as found for example by Papadimitrakis and Papaioannou (2003) in their analysis of data collected at several short fetch locations in the Aegean sea. They obtained: $A_2 = 0.04088$ and $B_2 = 1$, which then yield: $\xi = 23.76 \times 10^{-3} (c_p / u_*)^{-0.6}$.

Assuming that the value $\xi_{\text{max}} = 0.0356$ is an upper bound of (characteristic-average) wave slopes that describes realistic field conditions, and utilizing one (or all) of the above three ξ - c_p / u_* correlations, it is possible to determine the lower bound of wave age, $(c_p / u_*)_{\text{th}}$, below which it is expected that ξ will increase with increasing c_p / u_* . The values $(c_p / u_*)_{\text{th}} = 0.8, 0.5$ and 0.06

were obtained from the above three correlations with exponents: $-0.5, -0.6$ and -0.2424 , respectively. The least of these threshold values apparently corresponds to well developed-mature wave fields having large (dimensional and/or dimensionless fetches), while the former correspond to rather short fetches. It was felt that the value $(c_p / u_*)_{\text{th}} = 0.8$ is a reasonable lower limit of the validity of an inverse ξ - c_p / u_* relation. In fact, this value is closer to the threshold value $(c_p / u_*)_{\text{th}}$ that can be obtained by equating an expression for ξ similar to Eq. (4.1) of Huang et al. (1986) and that given by Kahma (1981), viz., $(4\pi\sqrt{2}\alpha_1)^{-1} \{1 - \alpha_0 (c_p / u_*)^{-1}\}^2 = 31.74 \times 10^{-3} (c_p / u_*)^{-0.5}$. Solution of the above equation, with $\alpha_0 \approx 0.5$, yields $(c_p / u_*)_{\text{th}} \approx 1.85$, but somewhat different values of c_p / u_* may be obtained if other α_0 values are used, in view of the various relations that describe the variation of α_0 with ξ and/or c_p / u_* . Lower values for $(c_p / u_*)_{\text{th}} (\leq 1.25)$ are obtained with the other two ξ - c_p / u_* correlations. The LHS and RHS expressions of the above equation describe the rising and falling branches of the ξ - c_p / u_* curve. Most investigators describe only the falling branch of this ξ - c_p / u_* curve.

References

- Baily, R.J., Jones, I.S.F., Toba, Y., 1991. The steepness and shape of wind waves. *Journal of Oceanographic Society of Japan* 47, 249–264.
- Banner, M.L., 1990. Equilibrium spectra of wind waves. *Journal of Physical Oceanography* 20, 984–996.
- Banner, M.L., Melville, W.K., 1976. On the separation of airflow over water waves. *Journal of Fluid Mechanics* 77, 825–842.
- Banner, M.L., Peregrine, D.H., 1993. Wave breaking in deep water. *Annual Review of Fluid Mechanics* 25, 373–397.
- Banner, M.L., Phillips, O.M., 1974. On the incipient breaking of small-scale waves. *Journal of Fluid Mechanics* 65, 647–656.
- Banner, M.L., Song, J.-B., 2002. On determining the onset and strength of breaking for deep-water waves. Part II: Influence of wind forcing and surface shear. *Journal of Physical Oceanography* 32, 2259–2570.
- Banner, M.L., Tian, X., 1998. Determining the onset of wave breaking for modulating surface gravity water waves. *Journal of Fluid Mechanics* 77, 2953–2956.
- Banner, M.L., Babanin, A.V., Young, I.R., 2000. Breaking probability for dominant waves on the sea surface. *Journal of Physical Oceanography* 30, 3145–3160.

- Banner, M.L., Gimmrich, J.R., Farmer, D.M., 2002. Multiscale measurements of Ocean wave breaking probability. *Journal of Physical Oceanography* 32, 3364–3375.
- Cartwright, D.E., Longuet-Higgins, M.S., 1956. The statistical distribution of the maximum of a random wave function. *Proceedings of the Royal Society of London* 237, 212–232.
- Cheung, T.K., 1985. A study of the turbulent boundary layer in the water at an air–water interface, Technical Report No. 287, Civil Engineering Department, Stanford University.
- Ding, L., Farmer, D.M., 1994. Observations of breaking wave statistics. *Journal of Physical Oceanography* 24, 1368–1387.
- Dold, J.W., Peregrine, D.H., 1986. Water-wave modulations. *Proceedings of the 20th International Conference on Coastal Engineering*, vol. 1, Taipei, Taiwan. ASCE, New York, 163–175.
- Donelan, M.A., Hamilton, J., Hui, W.H., 1985. Directional spectra of wind-generated waves. *Philosophical Transactions of the Royal Society of London A* 315, 509–562.
- Duncan, J.D., 2001. Spilling breakers. *Annual Review of Fluid Mechanics* 33, 517–547.
- Geernaert, G.L., Larsen, S.E., Hansen, F., 1987. Measurements of the wind stress, heat flux, and turbulence intensity during storm conditions over the North Sea. *Journal of Geophysical Research* 92 (C5), 13127–13139.
- Gemmrich, J.R., Farmer, D.M., 1999. Observations of the scale and occurrence of breaking surface waves. *Journal of Physical Oceanography* 29, 2595–2606.
- Glazman, R.E., 1986. Statistical characteristics of sea surface geometry for a wave field discontinuous in the mean square. *Journal of Geophysical Research* 91 (C5), 6629–6641.
- Holthuijsen, L.H., Herbers, T.H.C., 1986. Statistics of breaking waves observed as whitecaps in the open sea. *Journal of Physical Oceanography* 16, 290–297.
- Hsu, C.T., Wu, H.Y., Hsu, E.Y., Street, R.L., 1982. Momentum and energy transfer in wind generation of waves. *Journal of Physical Oceanography* 12, 929–951.
- Huang, N.E., Bliven, L.F., Long, S.R., Tung, C.C., 1986. An analytical model for oceanic whitecap coverage. *Journal of Physical Oceanography* 16, 1597–1604.
- Jones, I.S.F., Toba, Y., 2001. *Wind Stress Over the Ocean*. Cambridge University Press, Cambridge, 307pp.
- Kahma, K.K., 1981. A study of wave spectrum with fetch. *Journal of Physical Oceanography* 11, 1503–1515.
- Kahma, K.K., Calkoen, C.J., 1994. Growth curve observations. In: Komen, G.J., Cavaleri, L., Donelan, M., Hasselmann, K., Hasselmann, S., Janssen, P.A.E.M. (Eds.), *Dynamics and Modelling of Ocean Waves*. Cambridge University Press, Cambridge, pp. 74–82.
- Katsaros, K.B., Atakturk, S.S., 1991. Dependence of wave-breaking statistics on wind stress and wave development. In: Banner, M.L., Grimshaw, R.H.J. (Eds.), *Proceedings of the 1991 IUTAM Symposium*, Sydney, Australia, Springer, Berlin, 1991.
- Komen, G.J., 1987. Energy and momentum fluxes through the sea surface. *Proceedings of the Fourth “Aha Huliko” Workshop on: Dynamics of the Ocean Surface Mixed Layer*, January 14–16, pp. 207–217.
- Kinsman, B., 1965. *Wind waves: Their Generation and Propagation on the Ocean Surface*. Prentice-Hall, Englewood Cliffs, NJ, 676pp.
- Lake, B.M., Yuen, H.C., 1978. A new model for non-linear wind waves. Part 1. Physical model and experimental evidence. *Journal of Fluid Mechanics* 88, 33–62.
- Longuet-Higgins, M.S., 1957. The statistical analysis of a random, moving surface. *Philosophical Transactions of the Royal Society of London A* 249 (966), 321–387.
- Longuet-Higgins, M.S., 1962. The statistical geometry of random surfaces. *Hydrodynamic stability*. *Proceedings of the 13th Symposium on Applied Mathematics*. Providence, RI, American Mathematical Society, pp. 105–144.
- Longuet-Higgins, M.S., 1963. The generation of capillary waves by steep gravity waves. *Journal of Fluid Mechanics* 16 (3), 138–159.
- Longuet-Higgins, M.S., 1975a. Integral properties of periodic gravity waves of finite amplitude. *Proceedings of the Royal Society of London A* 342, 157–174.
- Longuet-Higgins, M.S., 1975b. On the joint distribution of the periods and amplitudes of sea waves. *Journal of Geophysical Research* 80 (C18), 2688–2694.
- Longuet-Higgins, M.S., 1980. The unsolved problem of breaking waves. *Proceedings of the 17th Conference on Coastal Engineering*, pp. 1–28.
- Longuet-Higgins, M.S., 1983. On the joint distribution of wave periods and amplitudes in a random wave field. *Philosophical Transactions of the Royal Society of London A* 389, 241–258.
- Longuet-Higgins, M.S., 1984. Statistical properties of wave groups in a random sea state. *Philosophical Transactions of the Royal Society of London A* 312, 219–250.
- Longuet-Higgins, M.S., 1985. Acceleration of steep gravity waves. *Journal of Physical Oceanography* 15, 1570–1579.
- Longuet-Higgins, M.S., 1986. Eulerian and Lagrangian aspects of surface waves. *Journal of Fluid Mechanics* 173, 683–707.
- Longuet-Higgins, M.S., Fox, M.J.H., 1978. Theory of the almost highest wave. Part 2. Matching and analytic extension. *Journal of Fluid Mechanics* 85, 769–786.
- Melville, K., 1996. The role of surface wave breaking in air–sea interaction. *Annual Reviews of Fluid Mechanics* 28, 279–321.
- Memos, C., 2002. Stochastic description of sea waves. *Journal of Hydraulic Research* 40 (3), 1–10.
- Memos, C., Tzani, K., 2000. Joint distribution of wave height and periods in waters of any depth. *Journal of Waterway, Port, Coastal, and Ocean Engineering* 126 (3), 162–172.
- Nepf, H.M., Wu, C.H., Chan, E.S., 1998. A comparison of two- and three-dimensional wave breaking. *Journal of Physical Oceanography* 28, 1496–1510.
- Ochi, M.K., Tsai, C.H., 1983. Prediction of occurrence of breaking waves in deep water. *Journal of Physical Oceanography* 13, 2008–2019.
- Papadimitrakis, Y.A., 1986. On the structure of artificially generated water wave trains. *Journal of Geophysical Research* 91 (D12), 14237–14249.

- Papadimitrakis, Y.A., Street, R.L., Hsu, E.Y., 1988. The bursting sequence in the turbulent boundary layer over progressive, mechanically-generated water waves. *Journal of Fluid Mechanics* 193, 303–345.
- Papadimitrakis, Y.A., Papaioannou, A., 2003. Sea surface roughness parameterization. In: Sajjadi, S.G., Hunt, J. (Eds.), *Wind over waves II: Forecasting and fundamentals of applications*. The Institute of Mathematics and Applications, Horwood Publishing, Chichester.
- Phillips, O.M., 1977. *The Dynamics of the Upper Ocean*. Cambridge University Press, Cambridge, NY, 336pp.
- Phillips, O.M., 1981. The dispersion of short wavelets in the presence of a dominant wave. *Journal of Fluid Mechanics* 107, 465–485.
- Phillips, O.M., 1985. Spectral and statistical properties of the equilibrium range in wind-generated gravity waves. *Journal of Fluid Mechanics* 156, 505–531.
- Plant, W.J., Wright, J.W., 1980. Phase speeds of upwind and downwind traversing short gravity waves. *Journal of Geophysical Research* 85 (C6), 3304–3310.
- Rapp, R., Melville, W.K., 1990. Laboratory measurements of deep-water breaking waves. *Philosophical Transactions of the Royal Society of London A* 331, 735–780.
- She, K., Greated, C.A., Easson, W.J., 1997. Experimental study of three-dimensional breaking Kinematics. *Applied Ocean Research* 19, 329–343.
- Smith, J., 1986. Short surface waves with growth and dissipation. *Journal of Geophysical Research* 91 (C2), 2616–2632.
- Snyder, R.L., Kennedy, R.M., 1983. On the formation of whitecaps by a threshold mechanism. Part I: Basic Formalism. *Journal of Physical Oceanography* 13, 1482–1492.
- Song, J.-B., Banner, M.L., 2001. On determining the onset and strength of breaking for deep water waves Part I: Unforced irrotational wave groups. *Journal of Physical Oceanography* 32, 2541–2558.
- Song, J.-B., Wu, Y.-H., 1999. Statistical distribution of maximum surface displacement in weakly nonlinear random waves. *Journal of Waterway, Port, Coastal, and Ocean Engineering* 125 (2), 59–65.
- Srokosz, M.A., 1986. On the probability of wave breaking in deep water. *Journal of Physical Oceanography* 16, 382–385.
- Tayfun, M.A., 1983. Effects of spectrum band width on the distribution of wave heights and periods. *Ocean Engineering* 10, 107–118.
- Thorpe, S.A., 1995. Dynamical processes of transfer at the sea surface. *Progress in Oceanography* 35, 315–352.
- Tulin, M.P., Li, J., 1992. On the breaking of energetic waves. *International Journal of Offshore Polar Engineering* 2, 46–53.
- Tulin, M.P., Waseda, T., 1999. Laboratory observations of wave group evolution, including breaking effects. *Journal of Fluid Mechanics* 378, 197–232.
- Tzani, K., 2003. Stochastic description of random sea states (Πιθανοτική περιγραφή τυχαίων κατάστασεων θαλάσσης). Ph.D. Thesis, National Technical University Athens, School of Civil Engineering, 271pp (in Greek).
- Vanmarcke, E., 1983. *Random Fields: Synthesis and Analysis*. MIT Press, Cambridge, MA, 382pp.
- Waseda, T., Tulin, M.P., 1999. Experimental study of the stability of deep-water wave trains including wind effects. *Journal of Fluid Mechanics* 401, 55–84.
- Wu, J., 1968. Laboratory studies of wind-wave interactions. *Journal of Fluid Mechanics* 34, 91–111.
- Xu, D., Huang, P.A., Wu, J., 1986. Breaking of wind-generated waves. *Journal of Physical Oceanography* 6, 2172–2178.
- Young, I.R., 1999. *Wind Generated Ocean Waves*. Elsevier, Amsterdam, The Netherlands, 288pp.
- Yuan, Y.L., 1982. On the statistical properties of sea waves. Ph.D. Thesis, North Carolina State University, Raleigh, NC.